Is a 6-Week Course of Ganciclovir Therapy Effective for Chorioretinitis in Infants with Congenital Cytomegalovirus Infection?

Kensuke Shoji, MD, Naoki Ito, MD, Yushi Ito, MD, Naoki Inoue, PhD, Shingo Adachi, MD, Takuya Fujimaru, MD, Tomoo Nakamura, MD, PhD, Sachiko Nishina, MD, PhD, Noriyuki Azuma, MD, PhD, and Akihiko Saitoh, MD, PhD

Effective treatment for chorioretinitis caused by congenital cytomegalovirus (CMV) infection remains unknown. We report an infant with congenital CMV infection, who required a 6-month course of antiviral therapy to control his chorioretinitis. Long-term treatment may be necessary for managing congenital CMV-associated chorioretinitis. *(J Pediatr 2010;157:331-3)*

Cytomegalovirus (CMV) is the most common cause of congenital infection in humans.[1] It has been shown that a 6-week course of intravenous ganciclovir (GCV) therapy prevents hearing deterioration in infants with symptomatic congenital CMV disease involving the central nervous system.[2] However, safe and effective treatment for chorioretinitis caused by congenital CMV infection is not yet established.[3] We recently experienced a case of congenital CMV-associated chorioretinitis, which required a 6-month course of antiviral therapy to be controlled.

See editorial, p 179 and related article, p 191

Case report

A 28-year-old mother was admitted to our neonatal intensive care unit because of intrauterine growth retardation of the fetus at 31 weeks of gestation. With fetal magnetic resonance imaging, enlargement of ventricles bilaterally and periventricular calcifications were demonstrated. Antenatal serologic testing at 32 weeks' gestational age had no remarkable findings, except for the presence of CMV-specific immunoglobulin (Ig) G.

The male infant was born at 38 weeks of gestational age. His weight, length, and head circumference were 2270 g (<10th percentile), 44 cm (<10th percentile), and 31 cm (10th percentile), respectively. Physical examination results were remarkable for petechiae on the entire body and hepatosplenomegaly. Complete blood count was within reference ranges except for thrombocytopenia (30 600/mm^3). Liver enzymes and kidney test results were within reference ranges. On the basis of these physical and laboratory findings, congenital infection was strongly suspected, and further evaluation was performed. With computed tomography of the head, enlargement of the ventricles bilaterally and remarkable bilateral periventricular calcifications were revealed. Although CMV-specific IgM was undetectable, CMV DNA was found in his blood and urine specimens collected on the fourth day of life with the real-time polymerase chain reaction assay described previously,[4] and CMV was isolated in human fibroblast cells from a urine specimen, confirming congenital CMV infection.

Ophthalmoscopic examination showed bilateral active chorioretinitis on the seventh day of life, which triggered treatment with intravenous GCV (12 mg/kg/day every 12 hours). His hospital course is summarized in the **Figure**. The patient tolerated a 6-week course of the GCV therapy well, and ophthalmoscopy indicated improvement of chorioretinitis without an active lesion. However, 2 weeks after discontinuation of the therapy, his chorioretinitis partially recurred, and GCV therapy with the same dose was reinitiated.

After restarting therapy, chorioretinitis improved gradually. Although active lesions of chorioretinitis were diminished, the presence of some exudates suggested incomplete stabilization. As a result, intravenous GCV was administrated for a total of 9 weeks and subsequently switched to oral valganciclovir (Val-GCV; 32 mg/kg/day every 12 hours) for the duration of therapy. The peak concentrations of GCV in serum specimens before and after changing to the Val-GCV therapy were 3.9 μg/dL and 6.6 μg/dL, respectively. Oral Val-GCV treatment was continued for 7 weeks. After the completion of the therapies, ophthalmoscopy did not identify any signs of recurrence of chorioretinitis.

In addition to chorioretinitis, the patient had hearing impairment (ABR measurements of the left and right ears were 80 dB and 105 dB, respectively) at the beginning of initial GCV treatment, and significant recovery of hearing of the

CMV	Cytomegalovirus
GCV	Ganciclovir
Ig	Immunoglobulin
Val-GCV	Valganciclovir

From the Division of General Pediatrics, Department of Interdisciplinary Medicine (K.S., S.A., T.F.), Division of Neonatology, Department of Maternal and Perinatal Services (N.Ito, Y.I., T.N.), National Center for Child Health and Development, Tokyo Japan; Department of Virology I, National Institute of Infectious Diseases, Tokyo, Japan (N.Inoue); and Division of Ophthalmology, Department of Surgical Subspecialties (S.N., N.A.), and Division of Infectious Disease, Department of Medical Subspecialties (A.S.), National Center for Child Health and Development, Tokyo, Japan.

Supported by a grant from the Ministry of Health and Welfare (H20-Kodomo-007 to Y.I. and N.Inoue). The authors declare no conflicts of interest.

 10.1016/j.jpeds.2010.02.020

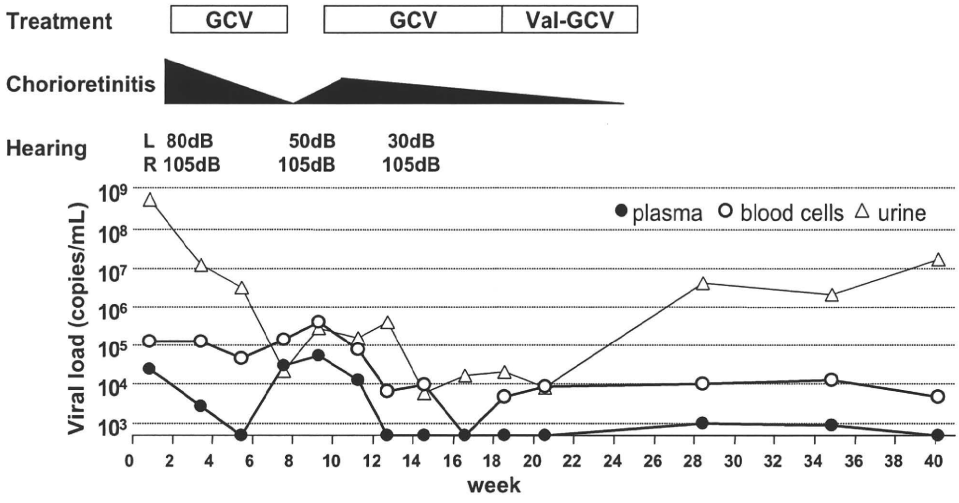

Figure. Summary of clinical manifestations and treatment are depicted: visual and hearing impairment, antiviral treatments, and longitudinal changes in cytomegalovirus viral loads in the urine, blood cells, and plasma specimens measured with the real-time polymerase chain reaction assay.

better ear (left, 30 dB; right, 105 dB) was observed after the initial GCV therapy; hearing level remained the same 6 month after the cessation of Val-GCV therapy. There were no adverse effects because of GCV and Val-GCV treatments in the patient; absolute neutrophil counts were examined at least once a week during the 6 months of antiviral therapy and remained within the reference range. Neurodevelopment was delayed, and he required anti-epileptic medication to control seizures; however, his eye and ear abnormalities were improved during long-term antiviral treatment. The patient was discharged from our hospital at 7 months of life. The last examination 1 year after the completion of antiviral therapy demonstrated that his ophthalmologic condition remained stable without active lesions.

Discussion

A 6-week course of GCV therapy has been used for a symptomatic infant with congenital CMV to prevent progression of hearing loss.[2] A clinical trial to compare a 6-month course with a 6-week course of Val-GCV therapy is under way to assess safety and efficacy characteristics (ClinicalTrials.gov NCT00466817).[5] Appropriate treatment for congenital CMV-associated chorioretinitis has not been well established.[3] To our knowledge, there are only a few reports in the literatures describing antiviral therapies for active chorioretinitis in patients with congenital CMV (**Table**).[2,6-12] Initial therapies to control CMV chorioretinitis ranged from 2 to 7 weeks. Some reports showed treatment benefits for CMV retinitis, but other reports demonstrated no treatment benefit.[2,14] A few reports demonstrated that longer duration of therapy up to 3 months was necessary to control chorioretinitis.[6] Clinical outcomes of patients differ significantly in different reports. Factors influencing clinical outcomes of patients may include: time to diagnosis, time to initiate GCV therapy, host factors to control CMV retinitis, and possibly the length of GCV therapy.

For long-term GCV therapy of congenital CMV, it is important to consider the most effective and least invasive toxic antiviral regimen. Kimberlin et al reported that a 16-mg/kg/dose of oral Val-GCV solution administered twice daily provided GCV exposure comparable with that of 6 mg/kg/dose of GCV intravenously.[13] Applying these novel data, we changed treatment from GCV intravenously (12 mg/kg/day, divided every 12 hours) to Val-GCV orally (32 mg/kg/day, dividied every 12 hours). Our pharmacokinetic data also confirmed that oral Val-GCV dose was sufficient to achieve the GCV level equivalent to that of the intravenous GCV administration.

The major toxicity in patients receiving GCV is hematologic abnormalities, notably neutropenia.[14] However, the incidence of neutropenia in congenital CMV infected infants varies significantly. For example, in the clinical trial conducted by Kimberlin et al, neutropenia developed in 63% of infants with congenital CMV infection who received GCV during the first 6 weeks of treatment.[2] For the GCV-induced neutropenia, it has been demonstrated that granulocyte colony stimulation factor could be used to increase the absolute neutrophil count, while continuing long-term GCV therapy.[2] However, Tanaka-Kitajima et al reported that neutropenia did not develop in any of 6 Japanese cases of congenital CMV during GCV treatment in a small and uncontrolled cohort study.[11] Similarly, Nigro et al found neutropenia only in 1 of 12 cases of congenital CMV treated with GCV.[6] In our case, neutropenia did not develop in the patient during the entire course of therapy, which allowed long-term administration of the drugs. It would be useful to identify any indicator, especially host factors, predictive of neutropenia in GCV therapy. GCV is known to cause gonadal toxicity and carcinogenicity in animal models,[15] and long-term

Table. Reports on treatment and outcome of chorioretinitis caused by congenital cytomegalovirus infection

Authors	Number of cases	Antiviral regimen, dosage and frequency	Duration	Clinical outcome of chorioretinitis	References
Kimberlin et al	8	GCV 6 mg/kg/dose X2/day or no treatment	6 weeks	no change	2
Nigro et al	3	GCV 5 mg/kg/dose X2/day	2 weeks	no change	6
	2	GCV 7.5 mg/kg/dose X2/day	2 weeks	resolution	
		GCV 10 mg/kg/dose X3/wk	3 months		
Coats et al	1	GCV (dose unknown)	Unknown	resolution > stabilization	7
Baumal et al	1	GCV 5 mg/kg/dose X2/day	4 weeks	complete regression of active retinitis	8
Barampouti et al	1	GCV 5 mg/kg/day	3 weeks	resolution	9
Weng et al	1	GCV 5 mg/kg/dose X3/day + Anti-CMV immunoglobulin 400 mg/kg/dose every other day	3 weeks 20 days	resolution	10
Tanaka-Kitajima et al	5	GCV 2.5-6 mg/kg/dose X2/day	2-7 weeks*	4/5 (80%) resolution 1/5 (20%) stabilization	11
Whitley et al.	14	GCV 4 or 6 mg/kg/dose X2/day	6 weeks	8/14 (57%) resolution 6/14 (43%) consequences 3: retinal detachment, 2: optic atrophy, 1: retinal hemorrhage	12

*One patient required 3 additional series of GCV therapy intravenously.

effects in humans are not established. Thus, further follow-up is necessary for such infants who required long-term GCV or Val-GCV therapy. ■

We acknowledge Drs Satoshi Hayashi and Haruhiko Sago at the Division of Perinatal Diagnosis for the perinatal diagnosis, Drs Noriko Morimoto and Hidenobu Taichi at the Division of Otolaryngology for hearing evaluation at the National Center for Child Health and Development, and Drs Hiroyuki Nakamura and Shigeyoshi Fujiwara at the Department of Infectious Diseases, National Research Institute for Child Health and Development, for coordinating the sample processing.

Submitted for publication Oct 7, 2009; last revision received Dec 29, 2009; accepted Feb 16, 2010.

Reprint requests: Akihiko Saitoh, MD, PhD, FAAP, 2-10-1 Okura, Setagaya-ku, Tokyo 157-0074 Japan. E-mail: saitoh-aki@ncchd.go.jp.

References

1. Kenneson A, Cannon MJ. Review and meta-analysis of the epidemiology of congenital cytomegalovirus (CMV) infection. Rev Med Virol 2007;17: 253-76.
2. Kimberlin DW, Lin CY, Sanchez PJ, Demmler GJ, Dankner W, Shelton M, et al. Effect of ganciclovir therapy on hearing in symptomatic congenital cytomegalovirus disease involving the central nervous system: a randomized, controlled trial. J Pediatr 2003;143:16-25.
3. Noffke AS, Mets MB. Spontaneous resolution of cytomegalovirus retinitis in an infant with congenital cytomegalovirus infection. Retina 2001; 21:541-2.
4. Ogawa H, Suzutani T, Baba Y, Koyano S, Nozawa N, Ishibashi K, et al. Etiology of severe sensorineural hearing loss in children: independent impact of congenital cytomegalovirus infection and GJB2 mutations. J Infect Dis 2007;195:782-8.
5. Nassetta L, Kimberlin D, Whitley R. Treatment of congenital cytomegalovirus infection: implications for future therapeutic strategies. J Antimicrob Chemother 2009;63:862-7.
6. Nigro G, Scholz H, Bartmann U. Ganciclovir therapy for symptomatic congenital cytomegalovirus infection in infants: a two-regimen experience. J Pediatr 1994;124:318-22.
7. Coats DK, Demmler GJ, Paysse EA, Du LT, Libby C. Ophthalmologic findings in children with congenital cytomegalovirus infection. J AAPOS 2000;4:110-6.
8. Baumal CR, Levin AV, Read SE. Cytomegalovirus retinitis in immunosuppressed children. Am J Ophthalmol 1999;127:550-8.
9. Barampouti F, Rajan M, Aclimandos W. Should active CMV retinitis in non-immunocompromised newborn babies be treated? Br J Ophthalmol 2002;86:248-9.
10. Weng YH, Chu SM, Lien RI, Chou YH, Lin TY. Clinical experience with ganciclovir and anti-cytomegalovirus immunoglobulin treatment for a severe case of congenital cytomegalovirus infection. Chang Gung Med J 2003;26:128-32.
11. Tanaka-Kitajima N, Sugaya N, Futatani T, Kanegane H, Suzuki C, Oshiro M, et al. Ganciclovir therapy for congenital cytomegalovirus infection in six infants. Pediatr Infect Dis J 2005;24:782-5.
12. Whitley RJ, Cloud G, Gruber W, Storch GA, Demmler GJ, Jacobs RF, et al. Ganciclovir treatment of symptomatic congenital cytomegalovirus infection: results of a phase II study. National Institute of Allergy and Infectious Diseases Collaborative Antiviral Study Group. J Infect Dis 1997; 175:1080-6.
13. Kimberlin DW, Acosta EP, Sanchez PJ, Sood S, Agrawal V, Homans J, et al. Pharmacokinetic and pharmacodynamic assessment of oral valganciclovir in the treatment of symptomatic congenital cytomegalovirus disease. J Infect Dis 2008;197:836-45.
14. Biron KK. Antiviral drugs for cytomegalovirus diseases. Antiviral Res 2006;71:154-63.
15. Marshall BC, Koch WC. Antivirals for cytomegalovirus infection in neonates and infants: focus on pharmacokinetics, formulations, dosing, and adverse events. Paediatr Drugs 2009;11:309-21.

STEM CELLS AND DEVELOPMENT
Volume 19, Number 11, 2010

DOI: 10.1089/scd.2010.0066

p38 Mitogen-Activated Protein Kinase Controls a Switch Between Cardiomyocyte and Neuronal Commitment of Murine Embryonic Stem Cells by Activating Myocyte Enhancer Factor 2C-Dependent Bone Morphogenetic Protein 2 Transcription

Jinzhan Wu,[1,2,*] Junko Kubota,[2,*] Jun Hirayama,[3,*] Yoko Nagai,[1,2] Sachiko Nishina,[4] Tadashi Yokoi,[1,4] Yoichi Asaoka,[1] Jungwon Seo,[1,2] Nao Shimizu,[1,2] Hiroaki Kajiho,[2] Takashi Watanabe,[5] Noriyuki Azuma,[4] Toshiaki Katada,[2] and Hiroshi Nishina[1]

Many studies have shown that it is possible to use culture conditions to direct the differentiation of murine embryonic stem (ES) cells into a variety of cell types, including cardiomyocytes and neurons. However, the molecular mechanisms that control lineage commitment decisions by ES cells remain poorly understood. In this study, we investigated the role of the 3 major mitogen-activated protein kinases (MAPKs: extracellular signal-regulated kinase, c-Jun N-terminal kinase, and p38) in ES cell lineage commitment and showed that the p38 MAPK-specific inhibitor SB203580 blocks the spontaneous differentiation of ES cells into cardiomyocytes and instead induces the differentiation of these ES cells into neurons. Robust p38 MAPK activity between embryoid body culture days 3 and 4 is crucial for cardiomyogenesis of ES cells, and specific inhibition of p38 MAPK activity at this time results in ES cell differentiation into neurons rather than cardiomyocytes. At the molecular level, inhibition of p38 MAPK activity suppresses the expression of *bmp-2* mRNA, whereas treatment of ES cells with bone morphogenetic protein 2 (BMP-2) inhibits the neurogenesis induced by SB203580. Further, luciferase reporter assays and chromatin immunoprecipitation experiments showed that BMP-2 expression in ES cells is regulated directly by the transcription factor myocyte enhancer factor 2C, a well-known substrate of p38 MAPK. Our findings reveal the molecular mechanism by which p38 MAPK activity in ES cells drives their commitment to differentiate preferentially into cardiomyocytes, and the conditions under which these same cells might develop into neurons.

Introduction

Murine embryonic stem (mES) cells are stem cells derived from the inner cell mass of embryonic day 3.5 (E3.5) blastocysts [1,2]. In the presence of leukemia inhibitory factor (LIF), mES cells can be maintained in an undifferentiated state *in vitro* and retain their potential for unlimited proliferation [3,4]. When LIF is removed from the culture and appropriate induction conditions are applied, ES cells can be directed to differentiate *in vitro* into a variety of cell lineages, including cardiomyocytes and neurons [5]. In humans, therapeutic transplantation of ES cells or their derivatives has been proposed as a potential treatment for various diseases. However, the molecular mechanisms governing the commitment of ES cells to specific cell lineages remain poorly understood. Elucidation of these mechanisms would greatly improve the efficiency of applied ES cell differentiation approaches.

The extracellular signal-regulated kinases (ERKs), c-Jun N-terminal kinases (JNKs), and p38 kinases are the 3 major groups of mitogen-activated protein kinases (MAPKs) found in mammals [6,7]. ERK1 and ERK2 are widely expressed and

[1]Department of Developmental and Regenerative Biology, Medical Research Institute, [3]Medical Top Track Program, Medical Research Institute, Tokyo Medical and Dental University, Tokyo, Japan.
[2]Department of Physiological Chemistry, Graduate School of Pharmaceutical Sciences, University of Tokyo, Tokyo, Japan.
[4]Department of Ophthalmology, National Center for Child Health and Development, Tokyo, Japan.
[5]Department of Laboratory Medicine, Kyorin University School of Medicine, Tokyo, Japan.
*These authors contributed equally to this work.

involved in the regulation of meiosis, mitosis, and post-mitotic functions in differentiated cells. In contrast, the JNK enzymes are important for controlling cell survival and apoptosis. The p38 kinases, which regulate the expression of many cytokines, were first identified in lipopolysaccharide-stimulated murine macrophages and in a screen for drugs able to inhibit tumor necrosis factor-α-mediated inflammatory responses in human monocytes [8,9]. Immune system cells that encounter inflammatory cytokines respond by activating p38, and this MAPK then supports the activation of immune responses. Four different p38 isoforms, p38α, p38β, p38γ, and p38δ, have been identified in mammalian cells [10]. The p38α and p38β isoforms are expressed in murine heart, whereas p38γ and p38δ are expressed at low levels in this organ. Deletion of the p38α gene in mice leads to early embryonic lethality between E11.5 and E12.5 [11,12]. On the other hand, p38β gene-targeted mice are viable and exhibit no apparent health problems [13]. It has been demonstrated that p38α associates with the transcription factor myocyte enhancer factor 2C (MEF2C), which is a member of the MADS-box family [14]. Phosphorylation of MEF2C by p38 stimulates MEF2C's ability to activate transcription of its target genes. In mammals, there are 4 MEF2 family genes, namely MEF2A, MEF2B, MEF2C, and MEF2D, which form homo- and heterodimers and bind to the DNA consensus sequence $CTA(A/T)_4TA(G/A)$ [15,16]. This sequence is found in the promoter regions of numerous muscle-specific genes, as well as in genes induced by growth factors or stress. A major role of the MEF2C protein is to regulate muscle-specific gene expressions. For example, loss-of-function mutations in myocyte enhancer factor 2C (*mef2c*) severely disrupt early cardiogenesis [17] and vascular development [18], suggesting that MEF2C may be critical for cardiomyogenesis by ES cells. However, the role of MEF2C in neural commitment is unknown.

Several extracellular signaling pathways are important for both embryonic and tissue stem cell determination, including pathways involving the Wnt proteins and the bone morphogenetic proteins (BMPs) [19,20]. However, a detailed understanding of the molecular mechanisms underlying the regulation of stem cell fate by these extracellular factors is lacking. BMPs are members of the transforming growth factor-β (TGF-β) superfamily and are known to function in the development and regulation of a wide range of biological systems. These extracellular ligands were originally isolated as components of bone extracts that induced ectopic cartilage and bone formation when implanted in muscle [21]. However, BMPs have since been demonstrated to function in multiple developmental processes, including dorsoventral patterning within the neural tube, the induction of mesoderm during gastrulation, and hematopoiesis [22]. As might be expected from these complex *in vivo* functions, BMPs also play key roles in regulating fate choices during tissue stem cell differentiation. For example, BMPs direct mesenchymal stem cells to differentiate into chondrogenic and osteogenic cell lineages [20]. BMPs have also been shown to regulate fate choices in neural crest stem cells [23].

In this study, we demonstrate that p38 MAPK controls an ES cell fate choice between cardiomyocytes and neurons. Further, our results show that this choice is mediated by the action of BMP-2, whose transcription is directly regulated by the p38 MAPK substrate MEF2C.

Materials and Methods

Cell culture and ES cell differentiation

Feeder cell-independent E14K ES cells were maintained on a gelatin-coated dish with Dulbecco's modified Eagle's medium (Gibco) containing 15% fetal bovine serum (FBS) (HyClone, Lot No. AMC15813), 0.1% 2-mercaptoethanol (Sigma), and 1000 U/mL LIF (propagation medium), as described previously [24–27]. To induce cardiomyocyte differentiation, LIF was removed from the propagation medium and 3×10^3 ES cells suspended in a 25 μL hanging drop. The drop was placed on the lid of an inverted bacterial Petri dish so that the cells would eventually attach and form embryoid bodies (EBs). After 2 days (on day 3), the EBs were collected and transferred into a bacterial Petri dish. After 4 days of suspension culture (on day 7), the EBs were plated on a gelatin-coated tissue culture dish. Areas of tissue showing a spontaneous "heartbeat" were readily detected on day 12.

For MAPK inhibition experiments, SB203580 (10 μM; Calbiochem), U0126 (10 μM; Promega), SP600125 (5 μM; Biomol), or wortmannin (1 μM; Wako) was added to EB cultures on day 1. For BMP-2 experiments, recombinant human BMP-2 (3 ng/mL; R&D Systems) or BMP-2 antagonist Noggin (100 ng/mL; R&D Systems) was added to EB culture on days 4–6.

Microscopic analysis of cardiomyocytes and neurons

Individual EBs, prepared as described earlier, were plated onto gelatin-coated 96-well tissue culture plates on day 7. The numbers of spontaneously beating EBs and EBs with neurite outgrowths were counted on day 12 under a phase-contrast microscope. Data were expressed as the percentage of the total number of EBs plated.

Immunofluorescence and immunohistochemistry

Immunofluorescence staining was performed as described previously [26]. For immunohistochemistry (IHC), EBs were fixed in 4% paraformaldehyde (PFA)–phosphate-buffered saline (PBS) for 2 h at 4°C, washed sequentially with PBS, 10% sucrose/PBS/0.02% NaN_3, 15% sucrose/PBS/0.02% NaN_3, and 20% sucrose/PBS/0.02% NaN_3, and embedded in OCT compound (Tissue Tek) with liquid nitrogen. Frozen sections were cut at 10 μm and placed on 3-aminopropyltriethoxy-silane (APES)-coated slides. After air drying, sections were fixed in acetone at room temperature for 10 min, rinsed in PBS, and incubated in 0.3% H_2O_2/PBS for 30 min to block endogenous peroxidases. After preincubation with blocking solution (5% bovine serum albumin/PBS/0.1% Tween 20) for 1 h, slides were incubated overnight at 4°C with a 1:800 dilution of anti-α-actinin antibody (cardiac specific) or a 1:500 dilution of anti-TuJ-1 (neuron-specific class III β-tublin) antibody. After 3×5 min washes in PBS/0.05% Tween 20 (PBST), sections were incubated with biotinylated secondary antibodies (Vectastain Elite ABC Kit) for 2 h. Slides were washed again in PBST and incubated for 1 h with Vectastain Elite ABC Reagent. Following a last wash in PBST, sections were incubated in 3,3′-Diaminobenzidine (DAB) solution (200 μg/mL DAB, 0.015% H_2O_2/PBS) until a color change was observed (2–10 min), and slides were rinsed in PBS. Finally, sections were counterstained with hematoxylin at room temperature for 1 min, washed, dehydrated, mounted, and inspected using a phase-contrast microscope.

Reverse transcriptase–polymerase chain reaction analysis

ES cells, EBs, or mouse organs (brain, heart, liver) from E12.5 mouse embryos were lysed with Trizol reagent (Invitrogen), and first-strand cDNA was synthesized using SuperScript III RNase H–reverse transcriptase (Invitrogen). The primers used in polymerase chain reactions (PCRs) are shown in Supplementary Table S1 (available online at www.liebertonline.com/scd).

Western blotting analysis

EBs were lysed and fractionated by sodium dodecyl sulfate–polyacrylamide gel electrophoresis and immunoblotted with antibody against total p38 (C-20; Santa Cruz Biotechnology) or phospho-p38 MAPK (Thr180/Tyr182) (Cell Signaling Technologies, No. 9211). Horseradish peroxidase-conjugated goat anti-rabbit IgG was used as the secondary antibody. Bands were observed using SuperSignal West Pico Chemiluminescent Substrate (Pierce) for total p38, or SuperSignal West Femto maximum sensitivity substrate (Pierce) for phospho-p38, as described previously [28].

Luciferase reporter assays

A proximal promoter region (−1703/−1) of mouse *bmp-2* containing the MEF2 binding site was amplified by PCR using the upstream primer 5′-CGACGCGTCTGTCCA GAGGCATCCATTT-3′ and the downstream primer 5′-CGCTCGAGAACACCTCCCCCTCGGA-3′. The sequence was confirmed and cloned into the pTAL-Luc reporter vector (pTAL-BMP-2-Luc). HeLa cells were cotransfected with pTAL-BMP-2-Luc and pcDNA3-Mef2c expressing MEF2C using FuGENE 6 transfection reagent (Roche Molecular Biochemicals). Luciferase activity was assayed at 24 h after transfection using the dual-luciferase reporter assay system (Promega) following the manufacturer's protocols.

Chromatin immunoprecipitation

Chromatin immunoprecipitation (ChIP) assays were performed according to published protocols from Cosmo Bio (http://www.cosmobio.co.jp) with minor modifications. EBs were fixed by adding 1% formaldehyde to the culture medium for 10 min at 25°C. Anti-MEF2C antibody (E-17; Santa Cruz Biotechnology) and control anti-actin IgG (I-19; Santa Cruz Biotechnology) were used to immunoprecipitate chromatin. The sequences of the ChIP primers were 5′-TCTG GAGTAGGTGGGTGTGG-3′ and 5′-CATGTGAGGGGACA ATGAGA-3′ for *bmp-2*; 5′-GGTGGGGAGAGAGCAGTTC-3′ and 5′-GTGAGATGCGTGATCCCTCT-3′ for *mef2c*; and 5′-GGAAAGGGGGTGTTGTTCTT-3′ and 5′-CCCTGACCATC ACCCTTCTA-3′ for the negative control gene bromo adjacent homology domain containing 1 (*bahd1*).

Results

The p38-specific inhibitor SB203580 and the ERK-specific inhibitor U0126 block spontaneous ES cell cardiomyogenesis

To identify the kinases most important for ES cell lineage commitment, we treated EBs with the ERK-specific inhibitor U0126, the JNK-specific inhibitor SP600125, the p38 MAPK-specific inhibitor SB203580, or the PI3K-specific inhibitor wortmannin. The inhibitors were applied to the EB cultures for the interval spanning days 1–6 during the EB differentiation process. We found that only the ERK-specific inhibitor U0126 and the p38 MAPK-specific inhibitor SB203580 blocked spontaneous cardiomyocyte differentiation, and that this block was so profound that fewer than 5% of EBs contained beating foci at day 12 (Fig. 1A). In contrast, more than 90% of untreated control EBs contained beating areas, which were confirmed as cardiac in commitment by phenotypic testing. Intriguingly, more than 90% of SB203580-treated EBs (but not U0126-treated EBs) continued to exhibit prominent outgrowths even though cardiomyogenesis was inhibited (Fig. 1B). These outgrowths stained positively with an anti-βIII-tubulin antibody specific for neurons, in contrast to the negative staining displayed by untreated EBs and EBs treated with U0126 (Fig. 1C, D). These results demonstrate that SB203580 blocks cardiomyocyte differentiation and induces neural differentiation, but that neural differentiation does not depend solely on the inhibition of cardiomyogenesis.

SB203580-mediated inhibition of p38 MAPK blocks cardiomyogenesis and commits ES cell differentiation to the neuronal lineage

To confirm that SB203580 had a switch effect on cardiac versus neural ES cell differentiation, frozen sections from EBs that had been untreated or treated with SB203580 between days 1 and 6 were subjected to IHC at day 12. SB203580-treated EBs did not stain positively with an antibody recognizing the cardiac-specific marker α-actinin, but did stain with an anti-TuJ-1 antibody specific for neurons (Fig. 2A). RT-PCR analysis of a set of embryonic genes revealed that SB203580 treatment completely inhibited the mRNA expression of the cardiac-associated *mef2c*, α-cardiac myosin heavy chain (*mhc*), and myosin light chain 2v (*mlc2v*) genes (Fig. 2B), but induced significant increases in the mRNA levels of the neuronal lineage genes *nestin*, hairy and enhancer of split 5 (*hes5*), mammalian achate schute homolog 1 (*mash1*), mouse atherosclerosis 3 (*math3*), and microtubule-associated protein 2 (*map2*) (Fig. 2C).

p38 MAPK activity between days 3 and 4 serves as a switch determining cardiac or neural commitment of ES cells

To define the role of p38 MAPK in ES cell commitment, we used immunoblotting to measure p38 MAPK activation during the earliest stages of ES cell differentiation. At day 0, when ES cells were cultured as a monolayer, no detectable phospho-p38 MAPK (activated enzyme) could be detected in whole cell lysates. However, after EB formation at day 2, high levels of phospho-p38 MAPK spontaneously appeared and were maintained until day 6; total p38 MAPK protein levels were not affected (Fig. 3A). To determine at what time point p38 MAPK acts during ES cell differentiation, we treated EBs with SB203580 for specific time intervals. As shown in Fig. 3B, when EBs were exposed to SB203580 between days 3 and 4, neuron differentiation was promoted at the expense of cardiomyocyte differentiation, an effect replicated by SB203580 treatment from day 0 to 6. In contrast, exposure to SB203580 for other intervals did not interfere

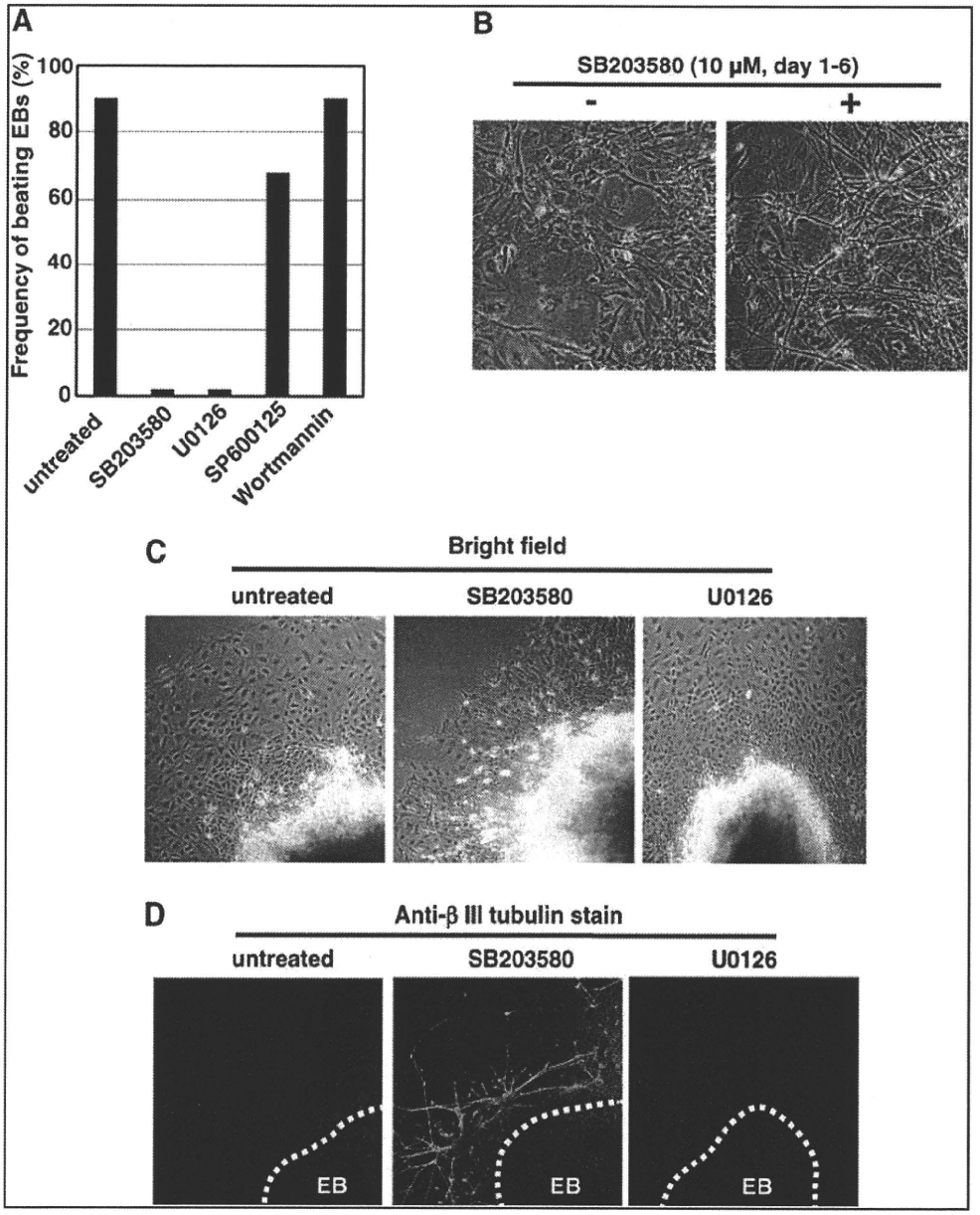

FIG. 1. Effects of specific mitogen-activated protein kinase inhibitors on embryonic stem (ES) cell differentiation. **(A)** Specific involvement of extracellular signal-regulated kinase (ERK) and p38 in cardiac differentiation. Embryoid bodies (EBs) were left untreated or treated with the p38-specific inhibitor SB203580 (10 μM), the ERK-specific inhibitor U0126 (10 μM), the c-Jun N-terminal kinase-specific inhibitor SP600125 (5 μM), or the PI3K-specific inhibitor wortmannin (1 μM) for the EB differentiation for the whole 6 days. Cardiomyocyte differentiation was determined by counting the number of EBs containing beating foci at day 12. Results are expressed as the mean percentage of total EBs plated. **(B)** Neurite outgrowths in the presence of SB203580. EBs were left untreated (−) or treated with 10 μM SB203580 (+) for days 1 − 6. Outgrowths were detected by photomicrography of EBs at day 12. **(C, D)** Neuronal differentiation. EBs were treated with SB203580 (p38) or U0126 (ERK) as in (A). On day 12, EB outgrowths were immunostained with anti-β-tubulin antibody specific for neuronal lineage cells and subjected to photomicrography. Bright field images by phase-contrast microscopy are shown. Dotted line: physical edge of EB in culture.

with spontaneous cardiomyocyte generation and did not induce neurogenesis. To examine dose-dependent effects of SB203580 on ES cell differentiation, we treated EBs with various concentrations of SB203580. As shown in Fig. 3C, when EBs were exposed to SB203580 between days 3 and 6, neuron differentiation was promoted at the expense of cardiomyocyte differentiation in a dose-dependent manner. RT-PCR analysis confirmed that the expression of the neuronal markers *hes5* and *map2* was induced only when SB203580 was applied to EBs between days 3 and 4, or between days 1 and 6, whereas expression of the cardiomyocyte-specific genes *mhc* and *mlc2v* was strongly decreased at these times

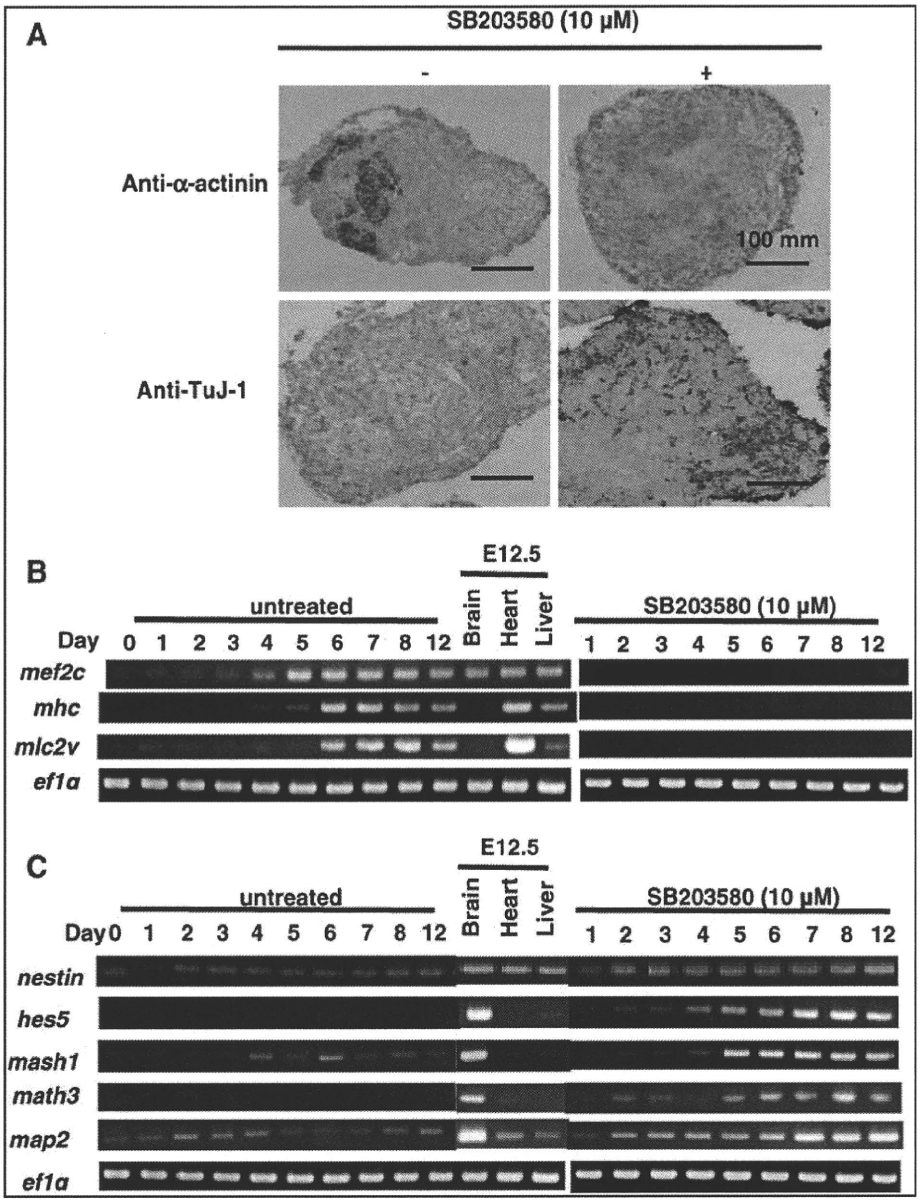

FIG. 2. SB203580-mediated inhibition of p38 mitogen-activated protein kinase blocks cardiomyogenesis and commits ES cells to the neuronal lineage. **(A)** Immunostaining. Embryoid bodies (EBs) were left untreated or treated with 10 μM SB203580 for days 1–6. EBs were harvested on day 7 and frozen sections were immunostained with anti-α-actinin antibody specific for cardiomyocytes or anti-TuJ-1 antibody specific for neurons. **(B)** Reduced cardiac gene expression. EBs were left untreated or treated with 10 μM SB203580 from day 1 until the indicated day, and extracts were analyzed by reverse transcriptase–polymerase chain reaction (RT–PCR) to detect mRNA expression of the cardiac-specific genes myocyte enhancer factor 2C (*mef2c*), α-cardiac myosin heavy chain (*mhc*), and myosin light chain 2v (*mlc2v*). Elongation factor 1α (*ef1a*) was used as the loading control. E12.5 brain, heart, and liver served as positive controls for the expression of various mRNAs. **(C)** Increased neuronal gene expression. EBs were left untreated or treated with 10 μM SB203580 from day 0 until the indicated day, and extracts were analyzed by RT-PCR to detect mRNA expression of the neuron-specific genes *nestin*, hairy and enhancer of split 5 (*hes5*), mammalian achate schute homolog 1 (*mash1*), *math3*, and microtubule-associated protein 2 (*map2*). Controls used were as same as for (B).

(Fig. 3C). These results clearly demonstrate that p38 MAPK activity spanning days 3 and 4 is critical for the cardiac commitment of ES cells, and that interference with this p38 MAPK activity drives neurogenesis instead.

p38 MAPK controls the expression of BMP-2 during ES cell differentiation

To elucidate the molecular mechanism by which p38 MAPK governs cell fate choices in ES cells, we sought to identify relevant downstream targets of this kinase. Because p38 MAPK activity spanning days 3 and 4 was found to be crucial for lineage commitment, we investigated whether the mRNA expression of genes known to be involved in ES cell fate decisions was affected by treating the EBs with SB203580 for this interval. Notably, RT-PCR analysis showed that the expression of the *bmp-2* mRNA, which normally commences on day 4, was decreased by SB203580 exposure compared with the untreated control (Fig. 4A). This effect was specific to *bmp-2* as none of the other genes examined showed any SB203580-induced difference in mRNA expression. Further analysis confirmed that *bmp-2* mRNA was first induced on day 4, and that SB203580 strongly repressed (but did not extinguish) this induction (Fig. 4B). On the other hand, U0126 did not repress the induction of *bmp-2* mRNA (Fig. 4C). These results indicate that p38 MAPK but not ERK regulates the induction of *bmp-2* mRNA in this ES cell differentiation.

BMP-2 inhibits SB203580-induced neuronal differentiation

To determine whether it was the downregulation of BMP-2 in SB203580-treated EBs that committed them to neurogenesis, we treated EBs that had been exposed to SB203580 on days 3–6 with recombinant human BMP-2 (rhBMP-2) on

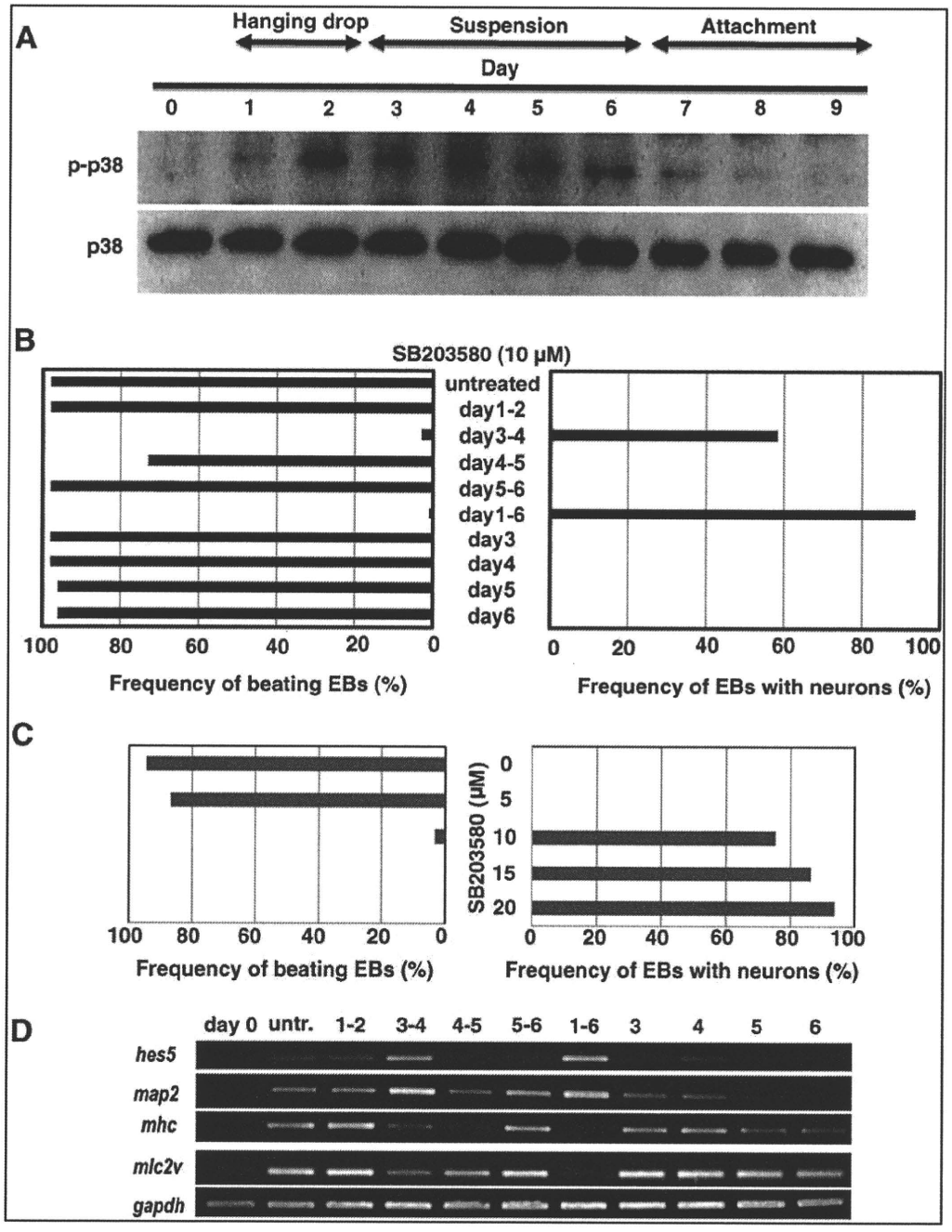

FIG. 3. p38 mitogen-activated protein kinase (MAPK) activity spanning days 3 and 4 serves as a switch determining cardiac or neuronal commitment of ES cells. **(A)** Spontaneous p38 MAPK activation spans days 2–6. Untreated embryoid bodies (EBs) were cultured from day 1 to 9, and whole cell extracts were subjected to Western blotting to detect phospho-p38 MAPK (p-p38, active enzyme) and total p38 MAPK protein (p38). **(B)** SB203580 treatment spanning days 3–4 induces switching. EBs were left untreated or treated with 10 μM SB203580 for the indicated time periods. On day 12, cardiomyocyte or neuronal differentiation was determined by counting numbers of EBs containing beating foci or showing neurite outgrowths. Results are expressed as the percentage of total EBs plated that showed cardiac or neuronal features. **(C)** Effects of SB203580 concentration on ES cell differentiation. EBs were left untreated or treated with the indicated concentrations of SB203580 from day 3 to 6. On day 12, cardiomyocyte or neuronal differentiation was determined as for (B). **(D)** Decreased cardiac but increased neuronal mRNAs. Extracts of the EBs in (B) were analyzed by reverse transcriptase (RT)–polymerase chain reaction to detect mRNA expression of cardiac-specific [α-cardiac myosin heavy chain (*mhc*), myosin light chain 2v (*mlc2v*)] and neuron-specific [hairy and enhancer of split 5 (*hes5*), microtubule-associated protein 2 (*map2*)] genes. Glyceraldehyde-3-phosphate dehydrogenase (*gapdh*), loading control; untr., untreated.

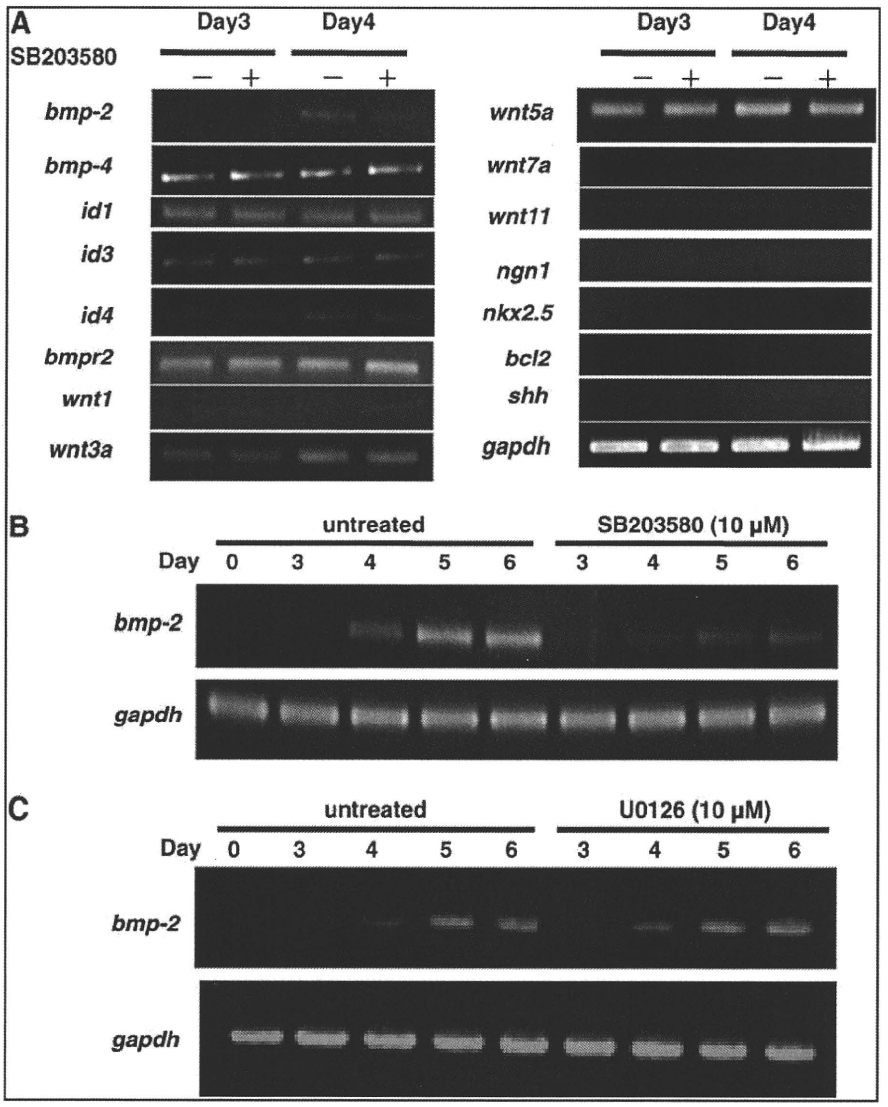

FIG. 4. p38 mitogen-activated protein kinase (MAPK) controls the expression of bone morphogenetic protein 2 (BMP-2) during ES cell differentiation. **(A)** SB203580 decreases *bmp-2* mRNA. Embryoid bodies (EBs) were left untreated or treated for days 3–4 with 10 μM SB203580. Extracts were analyzed by reverse transcriptase–polymerase chain reaction (RT–PCR) to evaluate transcript levels of the indicated cell fate-associated genes *bmp-2*, *bmp-4*, inhibitor of DNA binding 1 (*id1*), *id3*, *id4*, *bmp* receptor type II (*bmpr2*), wingless-type MMTV integration site family, member 1 (*wnt1*), *wnt3a*, *wnt5a*, *wnt7a*, *wnt11*, neurogenin 1 (*ngn1*), NK2 transcription factor related, locus 5 (*nkx2.5*), B-cell leukemia/lymphoma 2 (*bcl2*), and sonic hedgehog (*shh*). **(B, C)** p38 MAPK-mediated induction of *bmp-2* commences on day 4. EBs were left untreated or treated with 10 μM SB203580 or 10 μM U0126 on days 3–6 and *bmp-2* mRNA levels were determined by RT-PCR. Glyceraldehyde-3-phosphate dehydrogenase (gapdh) was used as the loading control.

days 4–6. As predicted, the neuronal differentiation induced by SB203580 treatment was dramatically repressed by rhBMP-2 treatment (Fig. 5A). A quantitative analysis showed that SB203580 treatment on days 3–6 induced nearly 80% of EBs to generate neuronal lineage cells, whereas the addition of rhBMP-2 on days 4–6 reduced this rate to fewer than 5% of EBs (Fig. 5B). Consistent with the microscopic analysis, RT-PCR confirmed that rhBMP-2 strongly inhibited SB203580-induced expression of the neuron-specific gene *map2* (Fig. 5C, top row). In contrast, expression levels of the cardiomyocyte-specific genes *mhc* and *mlc2v* in SB203580-treated EBs were not improved by the addition of rhBMP-2 (Fig. 5C, middle row).

The BMP-2 antagonist Noggin blocks cardiomyogenesis and induces neural differentiation

On the basis of the above results, we postulated that vigorous interference with endogenous BMP-2 function might prevent the differentiation of ES cells into cardiomyocytes and induce neurogenesis. To test this hypothesis, we treated EBs with the BMP-2 antagonist Noggin on days 4–6. Like SB203580 treatment, Noggin treatment of EBs at this time dramatically blocked cardiomyogenesis and promoted neuronal differentiation (Fig. 6A). A quantitative analysis showed that more than 60% of EBs treated with 100 ng/mL Noggin on days 4–6 differentiated into neurons, a rate similar to the 75% of EBs induced to undergo neurogenesis by SB203580 treatment on days 3–6 (Fig. 6B). Moreover, RT-PCR analysis confirmed that Noggin treatment strongly induced the expression of the neuronal gene *map2* and repressed expression of the cardiac gene *mhc* (Fig. 6C). Taken together, these results indicate that p38 MAPK controls ES cell lineage commitment (at least with respect to cardiomyocyte vs. neuron differentiation) by regulating the expression of BMP-2.

BMP-2 is a direct transcriptional target of MEF2C

The above experiments revealed that treatment of EBs with SB203580 resulted in a dramatic decrease in the mRNA expression of the transcription factor MEF2C, a well-known substrate of p38 MAPK (refer to Fig. 2B). We therefore compared the expression patterns of *mef2c* and *bmp-2* during

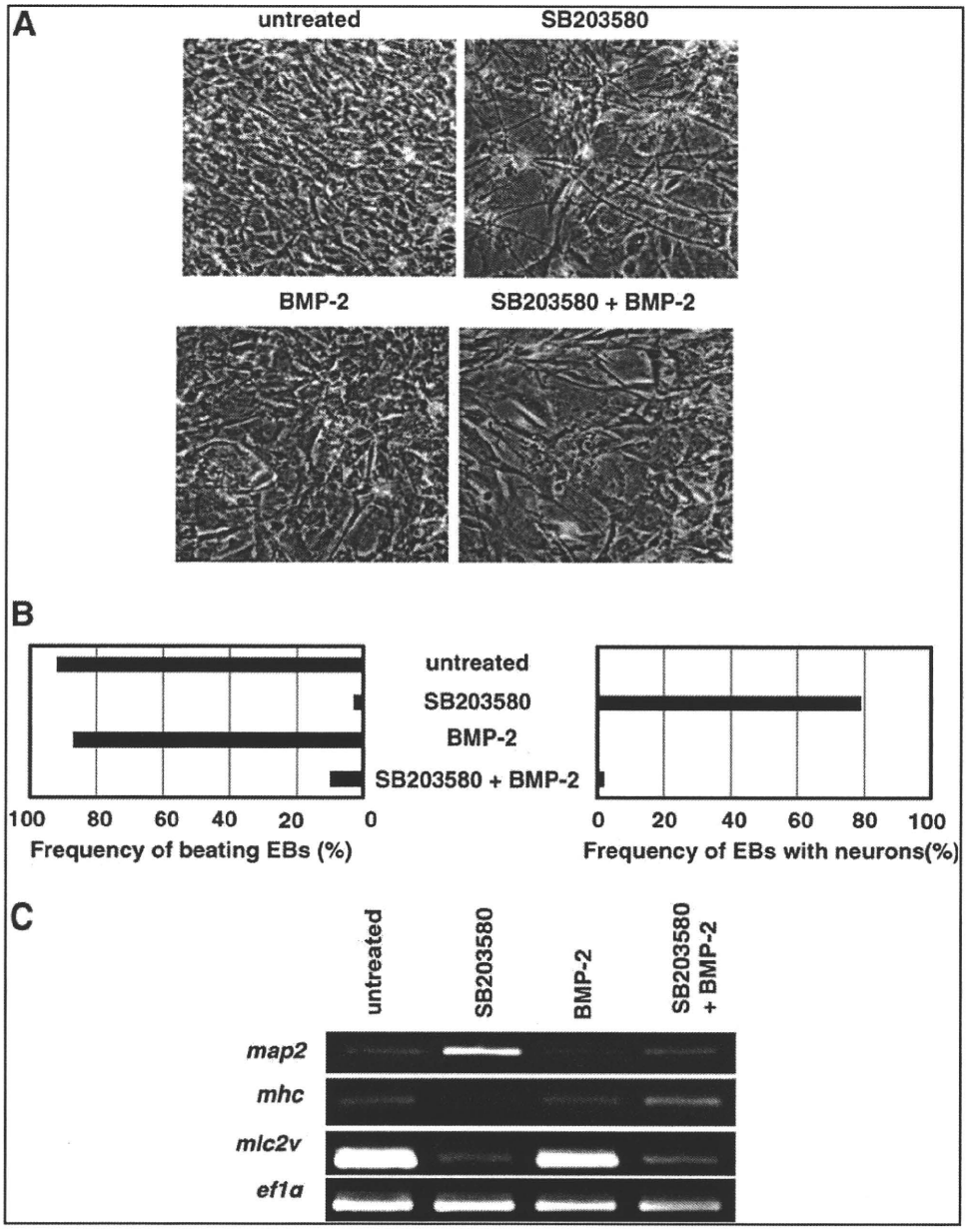

FIG. 5. Bone morphogenetic protein 2 (BMP-2) inhibits SB203580-induced neuronal differentiation. Embryoid bodies (EBs) were left untreated or treated with 3 ng/mL recombinant human BMP-2 on days 4–6 in the presence or absence of 10 μM SB203580 on days 3–6. **(A)** Outgrowth suppression. Photomicrographs of EBs at day 12 are shown. **(B)** Reduced frequency of EBs with neurons. EBs containing beating foci or neurite outgrowths were counted on day 12. Results are expressed as a percentage of EBs plated. **(C)** Increased cardiac but decreased neuronal mRNAs. Extracts of the EBs in (A) were analyzed by reverse transcriptase (RT)–polymerase chain reaction to determine mRNA levels of the indicated cardiac-specific [α-cardiac myosin heavy chain (*mhc*), myosin light chain 2v (*mlc2v*)] and neuronal [microtubule-associated protein 2 (*map2*)] genes. Elongation factor 1α (ef1α) was used as the loading control.

SB203580-induced neuronal differentiation and found that they were strikingly similar (Fig. 7A). Once activated by p38 MAPK-mediated phosphorylation, MEF2C activates the transcription of many cardiac-specific genes. Our observations suggested that p38 MAPK might induce BMP-2-regulated cardiomyogenesis by EBs via direct regulation of MEF2C. Importantly, a highly conserved consensus binding site for MEF2 has been identified in both the mouse and human proximal BMP-2 promoters. To test whether MEF2C could directly regulate BMP-2 transcription, we first carried out reporter assays in HeLa cells in which luciferase was placed under the control of a proximal region (−1703/−1 bp) of the mouse *bmp-2* promoter; this region contains the MEF2-binding site. HeLa cells engineered to overexpress MEF2C showed a 3-fold increase in luciferase activity, whereas SB203580 treatment repressed this transactivation (Fig. 7B).

To determine whether MEF2C could physically bind to the BMP2 promoter region, we carried out ChIP analyses of day

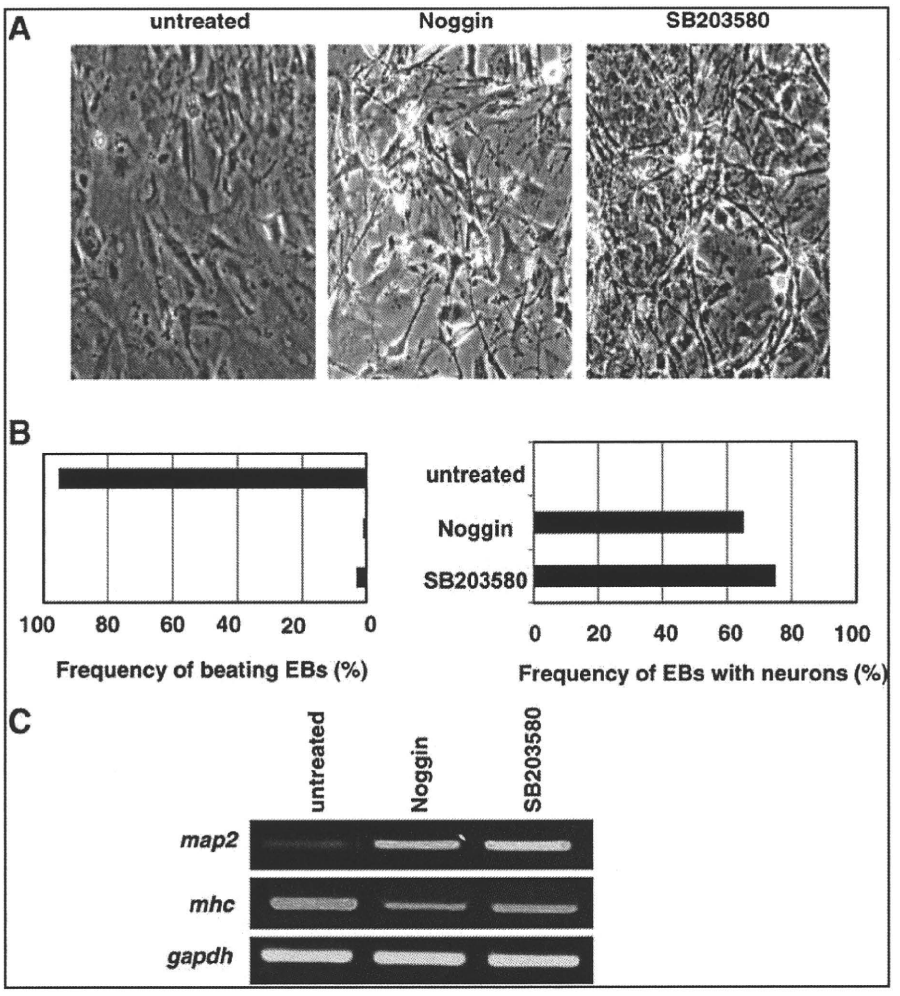

FIG. 6. The bone morphogenetic protein 2 antagonist Noggin blocks cardiomyogenesis and induces neuronal differentiation. Embryoid bodies (EBs) were left untreated or treated with 100 ng/mL Noggin on days 4–6, or with 10 μM SB203580 on days 3–6. **(A)** Outgrowth promotion. Photomicrographs of EBs at day 12 are shown. **(B)** Increased frequency of EBs with neurons. EBs containing beating foci or neurite outgrowths were counted on day 12. Results are expressed as a percentage of EBs plated. **(C)** Increased neuronal but decreased cardiac mRNAs. Extracts of the EBs in (A) were analyzed by reverse transcriptase–polymerase chain reaction (RT–PCR) to determine mRNA levels of the neuron-specific microtubule-associated protein 2 (*map2*) and cardiac-specific α-cardiac myosin heavy chain (*mhc*) genes. Glyceraldehyde-3-phosphate dehydrogenase (gapdh) was used as the loading control.

6 EBs that had been allowed to spontaneously differentiate. The region of the mouse *bmp-2* promoter encompassing the −656/−635 bp MEF2-binding site was successfully immunoprecipitated using anti-MEF2C antibody, indicating that MEF2C can indeed bind to the endogenous *bmp-2* promoter (Fig. 7C, top left panel). MEF2C did not bind to the promoter region of the control *bahd1* gene present on the same chromosome (Fig. 7C, top right). Further, SB203580 treatment inhibited the binding of MEF2C to the MEF2-binding site (Fig. 7C, bottom left). As a positive control, we examined the binding of MEF2C to the promoter of the mouse *mef2c* gene, which itself is a target of MEF2 transactivation. The resulting ChIP pattern was similar to that derived for *bmp-2* (Fig. 7C, middle). Collectively, these data indicate that BMP-2 is a direct transcriptional target of MEF2C.

Discussion

In this study, we analyzed the influence of the 3 major MAP kinases, ERK, JNK, and p38, on ES cell lineage commitment. Our results show that ERK and p38 MAPK play an essential role in the cardiomyogenesis of mES cells. An interesting cellular response of our work is that, at the same time as it promotes the induction of cardiomyocyte differentiation, p38 MAPK activity specifically inhibits neuronal differentiation. We demonstrate that p38 MAPK achieves these effects by activating the transcription factor MEF2C, which in turn directly regulates BMP-2 expression. Several previous studies also reported that p38 MAPK regulates both murine and human ES cell survival and lineage commitment, including cardiomyocyte differentiation [29–32]. Our work revealed the molecular mechanism of a switch between cardiomyocyte and neuronal commitment of mES cells.

The pyridinylimidazole compound SB203580 inhibits the catalytic activity of p38α and p38β MAPKs via competition for ATP, but SB203580 does not inhibit the closely related ERK or JNK enzymes or any other serine–threonine protein kinases [33]. Graichen *et al.* reported that SB203580 at concentrations lower than 10 μM induced cardiomyogenesis of human ES cells, whereas at concentrations more than 15 μM, it strongly inhibited cardiomyogenesis [30]. These results indicate the dose-dependent differences in lineage determination in human ES cells. However, we could not observe the phenomena using mES cells in the presence of SB203580 at concentrations of 5–20 μM (Fig. 3C). In our mES cell differentiation system, more than 90% EBs differentiated into cardiomyocytes in the absence of SB203580, and so it may be difficult to evaluate the enhanced induction of cardiomyogenesis by low concentrations of SB203580.

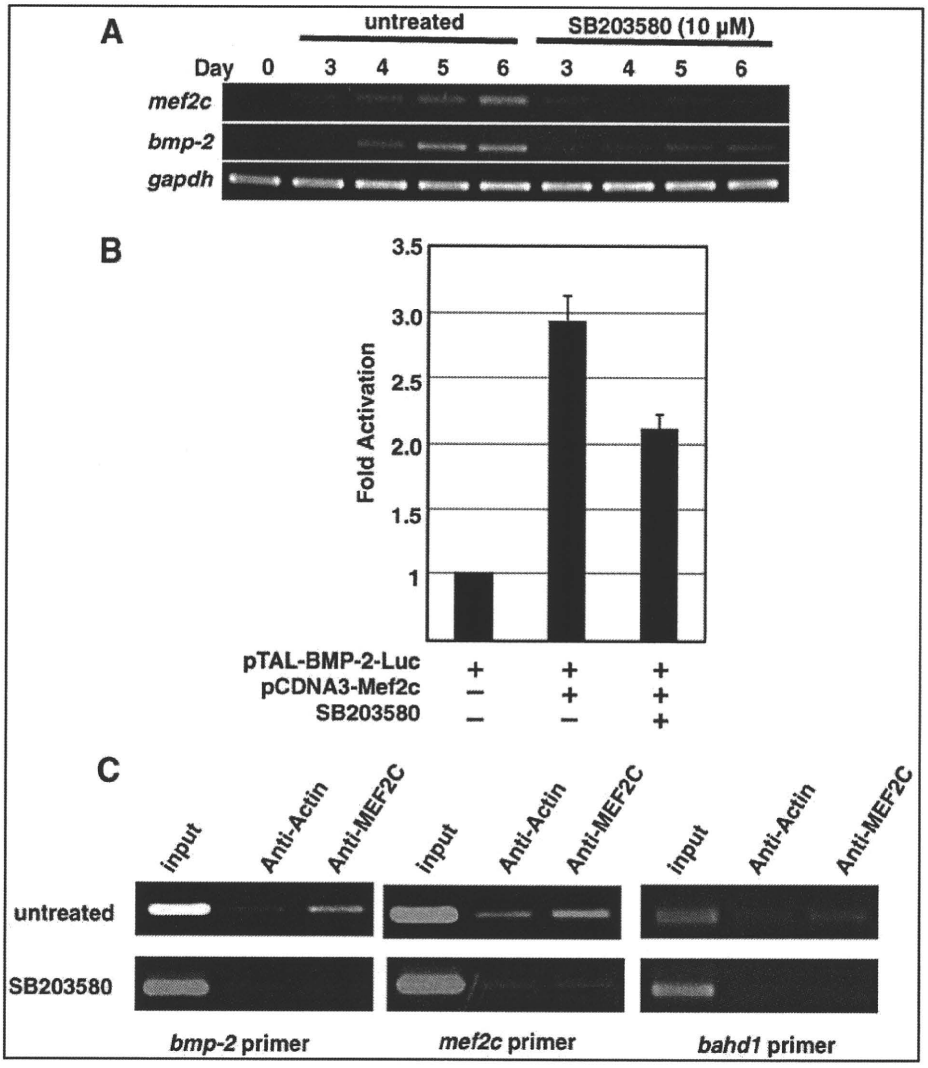

FIG. 7. Bone morphogenetic protein 2 (BMP-2) is a direct transcriptional target of myocyte enhancer factor 2C (MEF2C). **(A)** Similar patterns of *mef2c* and *bmp-2* expression. Embryoid bodies (EBs) were left untreated or treated with 10 μM SB203580 on days 3–6, and mRNA expression of *bmp-2* and *mef2c* was analyzed by reverse transcriptase–polymerase chain reaction (RT–PCR). Glyceraldehyde-3-phosphate dehydrogenase (gapdh) was used as the loading control. **(B)** MEF2C regulates *bmp-2* promoter activity. A proximal region (−1703/−1) of the mouse *bmp-2* promoter (containing the MEF2-binding site) was cloned into the pTAL-Luc reporter vector to yield pTAL-BMP-2-Luc, which was transfected into HeLa cells. HeLa cells were co-transfected with pcDNA3-Mef2c plasmid expressing MEF2C. Half of these co-transfected cells were treated with 10 μM SB203580. Luciferase activity was determined in cell lysates at 24 h after transfection. Results are expressed as the mean fold luciferase activation ± SD compared with pTAL-BMP-2-Luc-transfected HeLa cells. **(C)** MEF2C binds to the *bmp-2* promoter. EBs were left untreated or treated with 10 μM SB203580 on days 3–6. ChIP analyses of extracts were carried out on day 6 using anti-MEF2C antibody or control anti-actin IgG to immunoprecipitate chromatin. Precipitated DNAs were analyzed by PCR using primer pairs for the promoter regions of the *bmp-2*, *mef2c* (positive control), or bromo adjacent homology domain containing 1 (*bahd1*) (negative control) genes.

Consistent with our findings, Aouadi *et al.* have reported that loss of p38 MAPK activity due either to treatment with the chemical inhibitor PD169316 or to genetic p38α deficiency is sufficient to block cardiomyogenesis and induce a high level of neurogenesis [34]. These results clearly show that it is p38α that is mainly responsible for p38 MAPK functions during ES cell lineage commitment: the control of p38α activity constitutes an early switch, committing ES cells into either cardiomyogensesis (p38 on) or neurogenesis (p38 off). However, the molecular mechanism of p38 off-dependent neurogenesis was unclear.

P38 MAPK induces cell cycle exit and differentiation in many cell types, and activated p38 has been shown to phosphorylate several downstream signaling molecules important for cardiomyocyte differentiation and hypertrophy in murine P19 cells and mice [35–37]. In our study, we found that p38 MAPK is spontaneously activated between days 2 and 6 after the formation of EBs. Further, our data indicate that this spontaneous p38 MAPK activity is critical between days 3 and 4 for the cardiac commitment of ES cells. Inhibition of p38 MAPK activity at this early juncture drives ES cells toward the neuronal lineage. These findings stand in sharp contrast to those of other groups investigating the role of p38 MAPK in later stages of neuronal differentiation [38]. P38 MAPK activation is required for neurite formation and neuron survival in PC12 and P19 cells during the late stages of differentiation. Okamoto *et al.* reported that the p38α/MEF2 pathway prevents cell death during neuronal differentiation in P19 cells [39]. Thus, the role of p38 MAPK during the complex process of neuronal differentiation appears to be stage dependent.

BMPs are part of the larger superfamily of TGF-β ligands, which signal through a well-defined molecular pathway [21]. BMPs were found to be required for maintaining cultured mES cells in an undifferentiated state [40]. In our study, we demonstrate both that p38 MAPK regulates the expression of

BMP-2, and thereby controls mES cell lineage commitment, and that BMP-2 treatment inhibits SB203580-induced neuronal differentiation. Further, like SB203580, the exogenous BMP antagonist Noggin prevents the spontaneous differentiation of mES cells into cardiomyocytes and promotes neuronal differentiation. These data suggest a dynamic role for BMP in specifying cell fate and emphasize that defining the molecular context of BMP signaling is critical for understanding how ES cells are regulated at a physiological level.

MEF2C is an important transcription factor that transactivates many genes encoding cardiac structural proteins, and p38 MAPK is a well-known regulator of MEF2C [14,41–43]. Gene-targeted mouse embryos lacking MEF2C have cardiogenic defects [17]. BMP-2 is also required for cardiogenesis, and BMP2-deficient embryos exhibit an early defect in cardiac development [44]. In our study, we found that BMP-2 is a direct transcriptional target of MEF2C, and that p38 MAPK may regulate BMP-2 by controlling MEF2C activation. However, we found that simple stimulation of ES cells with BMP-2 did not augment cardiomyocyte generation (data not shown), suggesting that BMP-2 is essential but not sufficient for cardiac induction. It is likely that other MEF2C-dependent genes encoding cardiac structural proteins are also required for normal cardiac development. It will be interesting to investigate whether $MEF2C^{-/-}$ ES cells can differentiate spontaneously into neurons. Additionally, unknown factors in FBS contribute to the frequency of beating EBs and play important roles in cell lineage commitment.

In conclusion, our study has revealed an intriguing role for p38 MAPK as a cell fate switch during ES cell differentiation. The choice between cardiac and neuronal cell development depends on the early stage function of BMP-2, whose expression in turn depends on transactivation by the p38 MAPK target MEF2C.

Acknowledgments

This work was supported by research grants from the Ministry of Education, Culture, Sports, Science, and Technology of Japan and the Japanese Society for the Promotion of Science. The authors are grateful to numerous members of the Nishina and Katada Laboratories for critical reading of this manuscript and helpful discussions.

Author Disclosure Statement

No competing financial interests exist.

References

1. Evans MJ and M Kaufman. (1981). Establishment in culture of pluripotential cells from mouse embryos. Nature 292:154–156.
2. Martin GR. (1981). Isolation of a pluripotent cell line from early mouse embryos cultured in medium conditioned by teratocarcinoma stem cells. Proc Natl Acad Sci USA 78:7634–7638.
3. Smith AG, JK Heath, DD Donaldson, GG Wong, J Moreau, M Stahl and D Rogers. (1988). Inhibition of pluripotential embryonic stem cell differentiation by purified polypeptides. Nature 336:688–690.
4. Williams RL, DJ Hilton, S Pease, TA Willson, CL Stewart, DP Gearing, EF Wagner, D Metcalf, NA Nicola and NM Gough. (1988). Myeloid leukaemia inhibitory factor maintains the developmental potential of embryonic stem cells. Nature 336:684–687.
5. Smith AG. (2001). Embryo-derived stem cells: of mice and men. Annu Rev Cell Dev Biol 17:435–462.
6. Davis RJ. (2000). Signal transduction by the JNK group of MAP kinases. Cell 103:239–252.
7. Chang L and M Karin. (2001). Mammalian MAP kinase signalling cascades. Nature 410:37–40.
8. Han J, JD Lee, L Bibbs and RJ Ulevitch. (1994). A MAP kinase targeted by endotoxin and hyperosmolarity in mammalian cells. Science 265:156–160.
9. Lee JC, JT Laydon, PC McDonnell, TF Gallagher, S Kumar, D Green, D McNulty, MJ Blumenthal, JR Keys, SW Landvatter, JE Strickler, MM Mclaughlin, IR Siemens, SM Fisher, GP Livi, JR White, JL Adama and PR Young. (1994). A protein kinase involved in the regulation of inflammatory cytokine biosynthesis. Nature 372:739–746.
10. Wang XS, K Diener, CL Manthey, S Wang, B Rosenzweig, J Bray, J Delaney, CN Cole, PY Chan-Hui, N Mantlo, HS Lichenstein, M Zukowski and Z Yao. (1997). Molecular cloning and characterization of a novel p38 mitogen-activated protein kinase. J Biol Chem 272:23668–23674.
11. Tamura K, T Sudo, U Senftleben, AM Dadak, R Johnson and M Karin. (2000). Requirement for p38alpha in erythropoietin expression: a role for stress kinases in erythropoiesis. Cell 102:221–231.
12. Mudgett JS, J Ding, L Guh-Siesel, NA Chartrain, L Yang, S Gopal and MM Shen. (2000). Essential role for p38alpha mitogen-activated protein kinase in placental angiogenesis. Proc Natl Acad Sci USA 97:10454–10459.
13. Beardmore VA, HJ Hinton, C Eftychi, M Apostolaki, M Armaka, J Darragh, McIlrath J, JM Carr, LJ Armit, C Clacher, L Malone, G Kollias and JS Arthur. (2005). Generation and characterization of p38beta (MAPK11) gene-targeted mice. Mol Cell Biol 23:10454–10464.
14. Han J, Y Jiang, Z Li, VV Kravchenko and RJ Ulevitch. (1997). Activation of the transcription factor MEF2C by the MAP kinase p38 in inflammation. Nature 386:296–299.
15. Martin JF, JM Miano, CM Hustad, NG Copeland, NA Jenkins and EN Olson. (1994). A Mef2 gene that generates a muscle-specific isoform via alternative mRNA splicing. Mol Cell Biol 14:1647–1656.
16. Black BL and EN Olson. (1998). Transcriptional control of muscle development by myocyte enhancer factor-2 (MEF2) proteins. Annu Rev Cell Dev Biol 14:167–196.
17. Lin Q, J Schwarz, C Bucana and EN Olson. (1997). Control of mouse cardiac morphogenesis and myogenesis by transcription factor MEF2C. Science 276:1404–1407.
18. Bi W, CJ Drake and JJ Schwarz. (1999). The transcription factor MEF2C-null mouse exhibits complex vascular malformations and reduced cardiac expression of angiopoietin 1 and VEGF. Dev Biol 211:255–267.
19. Czyz J and A Wobus. (2001). Embryonic stem cell differentiation: the role of extracellular factors. Differentiation 68:167–174.
20. Tiedemann H, M Asashima, H Grunz and W Knöchel. (2001). Pluripotent cells (stem cells) and their determination and differentiation in early vertebrate embryogenesis. Dev Growth Differ 43:469–502.
21. Wozney JM, V Rosen, AJ Celeste, LM Mitsock, MJ Whitters, RW Kriz, RM Hewick and EA Wang. (1988). Novel regulators of bone formation: molecular clones and activities. Science 242:1528–1534.

22. Attisano L and JL Wrana. (2002). Signal transduction by the TGF-beta superfamily. Science 296:1646–1647.
23. Shah NM, AK Groves and DJ Anderson. (1996). Alternative neural crest cell fates are instructively promoted by TGFbeta superfamily members. Cell 85:331–343.
24. Nishina H, KD Fischer, L Radvanyi, A Shahinian, R Hakem, EA Rubie, A Bernstein, TW Mak, JR Woodgett and JM Penninger. (1997). Stress-signaling kinase Sek1 protects thymocytes from apoptosis mediated by CD95 and CD3. Nature 385:350–353.
25. Takayanagi H, S Kim, T Koga, H Nishina, M Isshiki, H Yoshida, A Saiura, M Isobe, T Yokochi, J Inoue, EF Wagner, TW Mak, T Kodama and T Taniguchi. (2002). Induction and Activation of the Transcription Factor NFATc1 (NFAT2) Integrate RANKL Signaling. Dev Cell 3:889–901.
26. Shimizu N, H Watanabe, J Kubota, J Wu, R Saito, T Yokoi, T Era, T Iwatsubo, T Watanabe, S Nishina, N Azuma, T Katada and H Nishina. (2009). Pax6-5a promotes neuronal differentiation of murine embryonic stem cells. Biol Pharm Bull 32:999–1003.
27. Saito R, T Yamasaki, Y Nagai, J Wu, H Kajiho, T Yokoi, E Noda, S Nishina, H Niwa, N Azuma, T Katada and H Nishina. (2009). CrxOS maintains self-renewal capacity of murine embryonic stem cells. Biochem Biophys Res Commun 390:1129–1135.
28. Ura S, H Nishina, Y Gotoh and Katada T. (2007). Activation of the JNK patyway by MST1 is essential and sufficient for the induction of chromatin condensation during apoptosis. Mol Cell Biol 27:5514–5522.
29. Androutsellis-Theotokis A, RR Leker, F Soldner, DJ Hoeppner, R Ravin, SW Poser, MA Rueger, SK Bae, R Kittappa and RD McKay. (2006). Notch signalling regulates stem cell numbers *in vitro* and *in vivo*. Nature 442:823–826.
30. Graichen R, X Xu, SR Braam, T Balakrishnan, S Norfiza, S Sieh, SY Soo, SC Tham, C Mummery, A Colman, R Zweigerdt and BP Davidson. (2008). Enhanced cardiomyogenesis of human embryonic stem cells by a small molecular inhibitor of p38 MAPK. Differentiation 76:357–370.
31. Binétruy B, L Heasley, F Bost, L Caron and M Aouadi. (2007). Concise review: regulation of embryonic stem cell lineage commitment by mitogen-activated protein kinases. Stem Cells 25:1090–1095.
32. Ding L, XG Liang, Y Hu, DY Zhu and YJ Lou. (2008). Involvement of p38MAPK and reactive oxygen species in icariin-induced cardiomyocyte differentiation of murine embryonic stem cells *in vitro*. Stem Cells Dev 17:751–760.
33. Cuenda A, J Rouse, YN Doza, R Meier, P Cohen, TF Gallagher, PR Young and JC Lee. (1995). SB 203580 is a specific inhibitor of a MAP kinase homologue which is stimulated by cellular stresses and interleukin-1. FEBS Lett 364:229–233.
34. Aouadi M, F Bost, L Caron, K Laurent, Y Le Marchand Brustel and B Binétruy. (2006). p38 mitogen-activated protein kinase activity commits embryonic stem cells to either neurogenesis or cardiomyogenesis. Stem Cells 24:1399–1406.
35. Davidson SM and M Morange. (2000). Hsp25 and the p38 MAPK pathway are involved in differentiation of cardiomyocytes. Dev Biol 218:146–160.
36. Zetser A, E Gredinger and E Bengal. (1999). p38 mitogen-activated protein kinase pathway promotes skeletal muscle differentiation. Participation of the Mef2c transcription factor. J Biol Chem 274:5193–5200.
37. Liang Q and JD Molkentin. (2003). Redefining the roles of p38 and JNK signaling in cardiac hypertrophy: dichotomy between cultured myocytes and animal models. J Mol Cell Cardiol 35:1385–1394.
38. Takeda K and H Ichijo. (2002). Neuronal p38 MAPK signalling: an emerging regulator of cell fate and function in the nervous system. Genes Cells 7:1099–1111.
39. Okamoto S, D Krainc, K Sherman and SA Lipton. (2000). Antiapoptotic role of the p38 mitogen-activated protein kinase-myocyte enhancer factor 2 transcription factor pathway during neuronal differentiation. Proc Natl Acad Sci USA 97:7561–7566.
40. Ying QL, J Nichols, I Chambers and A Smith. (2003). BMP induction of Id proteins suppresses differentiation and sustains embryonic stem cell self-renewal in collaboration with STAT3. Cell 115:281–292.
41. Zhao M, L New, VV Kravchenko, Y Kato, H Gram, F di Padova, EN Olson, RJ Ulevitch and J Han. (1999). Regulation of the MEF2 family of transcription factors by p38. Mol Cell Biol 19:21–30.
42. Yang SH, A Galanis and AD Sharrocks. (1999). Targeting of p38 mitogen-activated protein kinases to MEF2 transcription factors. Mol Cell Biol 19:4028–4038.
43. Wu Z, PJ Woodring, KS Bhakta, K Tamura, F Wen, JR Feramisco, M Karin, JY Wang and PL Puri. (2000). p38 and extracellular signal-regulated kinases regulate the myogenic program at multiple steps. Mol Cell Biol 20:3951–3964.
44. Zhang H and A Bradley. (1996). Mice deficient for BMP2 are nonviable and have defects in amnion/chorion and cardiac development. Development 122:2977–2986.

Address correspondence to:
Prof. Hiroshi Nishina
Department of Developmental and Regenerative Biology
Medical Research Institute
Tokyo Medical and Dental University
1-5-45 Yushima, Bunkyo-ku
Tokyo 113-8510
Japan

E-mail: nishina.dbio@mri.tmd.ac.jp

Received for publication February 6, 2010
Accepted after revision April 22, 2010
Prepublished on Liebert Instant Online April 22, 2010

CLINICAL REPORT

AMERICAN JOURNAL OF medical genetics PART A

A De Novo Deletion of 20q11.2–q12 in a Boy Presenting With Abnormal Hands and Feet, Retinal Dysplasia, and Intractable Feeding Difficulty

Yoko Hiraki,[1,2] Akira Nishimura,[2] Michiko Hayashidani,[3] Yoshiko Terada,[4] Gen Nishimura,[5] Nobuhiko Okamoto,[6] Sachiko Nishina,[7] Yoshinori Tsurusaki,[2] Hiroshi Doi,[2] Hirotomo Saitsu,[2] Noriko Miyake,[2] and Naomichi Matsumoto[2]*

[1]Hiroshima Municipal Center for Child Health and Development, Hiroshima, Japan

[2]Department of Human Genetics, Yokohama City University Graduate School of Medicine, Yokohama, Japan

[3]Medical Center for Premature and Neonatal Infants, Hiroshima City Hospital, Hiroshima, Japan

[4]Department of Ophthalmology, Hiroshima City Hospital, Hiroshima, Japan

[5]Department of Pediatric Imaging, Tokyo Metropolitan Children's Medical Center, Tokyo, Japan

[6]Department of Medical Genetics, Osaka Medical Center and Research Institute for Maternal and Child Health, Osaka, Japan

[7]Department of Ophthalmology, National Center for Child Health and Development, Tokyo, Japan

Received 18 June 2010; Accepted 23 October 2010

Proximal interstitial deletions involving 20q11–q12 are very rare. Only two cases have been reported. We describe another patient with 20q11.21–q12 deletion. We precisely mapped the 6.5-Mb deletion and successfully determined the deletion landmarks at the nucleotide level. Common clinical features among the three cases include developmental delay, intractable feeding difficulties with gastroesophageal reflux, and facial dysmorphism including triangular face, hypertelorism, and hypoplastic alae nasi, indicating that the 20q11.2–q12 deletion can be a clinically recognizable syndrome. This is also supported by the fact that the three deletions overlap significantly. In addition, unique features such as arthrogryposis/fetal akinesia (hypokinesia) deformation and retinal dysplasia are recognized in the patient reported herein.

Key words: 20q interstitial deletion; abnormal hands and feet; retinal dysplasia; feeding difficulty

How to Cite this Article:
Hiraki Y, Nishimura A, Hayashidani M, Terada Y, Nishimura G, Okamoto N, Nishina S, Tsurusaki Y, Doi H, Saitsu H, Miyake N, Matsumoto N. 2011. A de novo deletion of 20q11.2–q12 in a boy presenting with abnormal hands and feet, retinal dysplasia, and intractable feeding difficulty.
Am J Med Genet Part A 155:409–414.

INTRODUCTION

Interstitial deletions of the long arm of chromosome 20 are rare. To our knowledge, a total of 12 patients have been reported in the literature [Petersen et al., 1987; Shabtai et al., 1993; Aldred et al., 2002; Genevieve et al., 2005; Callier et al., 2006; Borozdin et al., 2007; Iqbal and Al-Owain, 2007]. Among them, only two cases showed the proximal q deletion (20q11–q12), not extending to q13 [Callier et al., 2006; Iqbal and Al-Owain, 2007]. One patient had a 6.6-Mb deletion at 20q11.21–q11.23 [Callier et al., 2006], and the other [Iqbal and Al-Owain, 2007] showed a 6.8-Mb deletion at 20q11.2–q12. Here, we report on the third patient with a 6.5-Mb deletion at 20q11.21–q12, clinically showing mental retardation, minor craniofacial anomalies, and intractable feeding difficulties. The deletion has been precisely analyzed at the nucleotide level and his detailed clinical manifestations will be presented.

Grant sponsor: Japan Society for the Promotion of Science (JSPS); Grant sponsor: Ministry of Health, Labour and Welfare; Grant sponsor: Ministry of Education, Culture, Sports, Science and Technology of Japan; Grant sponsor: Scientific Research.

*Correspondence to:
Naomichi Matsumoto, Department of Human Genetics, Yokohama City University Graduate School of Medicine, Fukuura 3-9, Kanazawa-ku, Yokohama 236-0004, Japan. E-mail: naomat@yokohama-cu.ac.jp

Published online 11 January 2011 in Wiley Online Library (wileyonlinelibrary.com).
DOI 10.1002/ajmg.a.33818

CLINICAL REPORT

The 18-month-old boy was the first product of healthy 22-year-old mother and 25-year-old father without any consanguinity. Pregnancy was uneventful. Family history was unremarkable. He was born by spontaneous vaginal delivery at 38 weeks of gestation. Birth weight was 2,230 g (−1.7 SD), length 44.0 cm (−1.9 SD), and OFC 32.5 cm (−0.3 SD). Multiple malformations including patent ductus arteriosus, patency of foramen ovale, and dysmorphic face were noted. He was tube-fed due to poor swallowing and oxygen therapy was required until 4 months because of respiratory disturbance. X-ray examination at age of 1 month revealed small thorax and mild slender long bones. In addition, right eye retinal fold was pointed out. At age of 3 months, upper gastrointestinal tract was investigated because of recurrent vomiting, and gastroesophageal reflux (GER) and esophageal hiatus hernia were found. Esophageal hiatus hernia was alleviated spontaneously, but GER persisted.

At age of 4 months, he was referred to us for evaluation of his developmental delay. He was noted to have the following craniofacial features: triangular face, premature closure fontanelle, slopping forehead, wide bending eyebrows, hypertelorism, low-set and posterior rotated ears, long columella nasi, mild hypoplastic alae nasi, short and well-defined philtrum, thin lips with tucked-in lower lip, submucosal cleft palate, microretrognathia and posterior low hair-line (Fig. 1A,B and Table I). Additionally, abnormal hands and feet were recognized, consisted of restriction of all proximal interphalangeal joints and over-extension of all distal interphalangeal joints of hands and feet, radial deviation of 2nd fingers, clinodactyly of the 2nd and 5th fingers, lack of flexion creases bilaterally, right preaxial polydactyly, left single palmar, and talipes valgus. Mild restriction of elbow, hip and knee joints bilaterally was also noted (Fig. 1C–E and Table I).

At 15 months, his weight was 7.5 kg (−2.3 SD), length 71.8 cm (−2.7 SD), and OFC 44.4 cm (−1.6 SD). He could roll over one side and shift a toy from one hand to the other. Social smile was seen, but he could not recognize his parents (DQ 48). His dysphagia persisted based on the modified swallowing study [Kanda et al., 2005]; he required tube-feeding, and rejected oral intake. Ophthalmic examination at 15 months revealed broom-like pattern of retinal vessels extending from optic disc to periphery with a falciform retinal fold in the right eye, causing visual impairment. In the left eye, mild opacity in the lateral portion of vitreous body was found. These findings led to the diagnosis of bilateral retinal dysplasia. Anterior segment and optic disc were normal. Left hearing loss was suspected by auditory brainstem response, otoacoustic emission, and behavioral observation audiometry. Brain magnetic resonance imaging revealed cortical atrophy and mild ventriculomegaly. Blood biochemistry and abdominal ultrasonographic examination were all normal. Serological TORCH (toxoplasma, rubella, cytomegarovirus, and herpes simplex) testing was negative. At 18 months, the shortening of 5th middle phalanges of fingers and absence of middle phalanges of the toes were confirmed by X-ray examination.

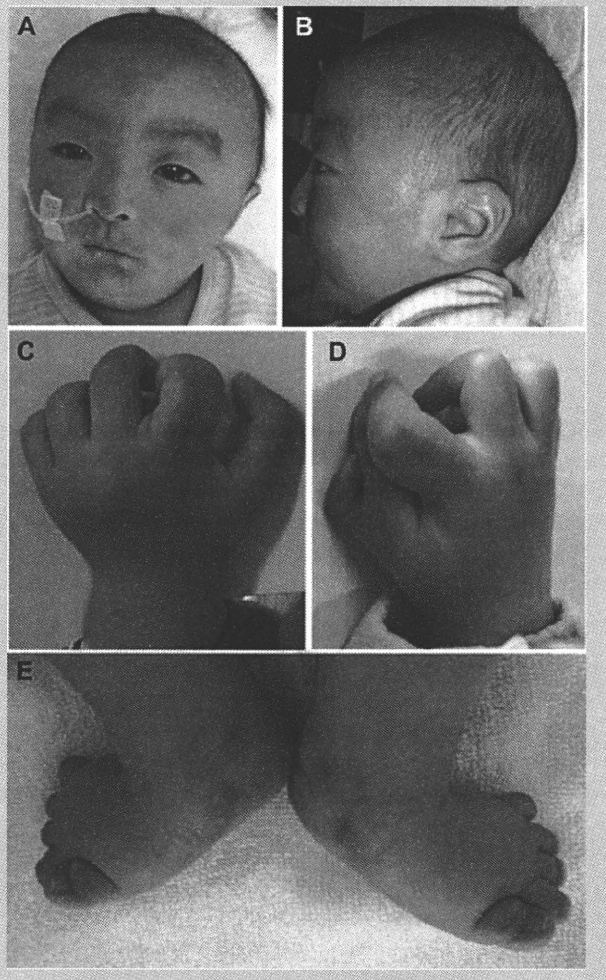

FIG. 1. Photographs of the patient at age of 4 months. A,B: Facial abnormalities including triangular face, wide and bending eyebrows, hypertelorism, long columella, thin lips with tucked-in lower lip, and microretrognathia were recognized. C (left hand) and D (right): Bilateral camptodactyly associated with radial deviation of the 2nd fingers and clinodactyly of the 2nd and 5th, and right preaxial polydactyly were noted. E: Camptodactyly with talipes valgus in both feet.

CYTOGENETIC AND MOLECULAR ANALYSIS

G-banded chromosomal analysis (550 bands level) of the patient's blood lymphocytes indicated normal karyptype (46,XY) (data not shown). Fluorescence in situ hybridization (FISH) analysis using all chromosomal subtelomeric clones did not show any abnormalities. Array CGH analysis using NimbleGen 385K Array (Roche NimbleGen, Inc., Madison, WI) demonstrated a 6.5-Mb heterozygous deletion at 20q11.2–q12 (UCSC genome coordinates 2006 Mar. version, chromosome 20: 31,269,661–37,782,841 bp) (Fig. 2A). The deletion was also confirmed by FISH using BACs (RP11-322B6 and RP11-782C16 at 21q11.21, and RP11-54P22 and RP11-467J15 at 20q12), RP11-787C16 and RP11-54P22 was deleted while RP11-322B6 and RP11-467J15 were not deleted (Fig. 3). The deletion junction was successfully amplified by PCR using primers (Primer A: 5′-TGA TAG AGC CAA CTG GGT CAT GTG C-3′, Primer C: 5′-TCT AGC TTG CTG AAT TCC TGC CTG A-3′) (Fig. 2B) and its product was sequenced. The deleted region was from 31,274,015 to 37,783,826 bp (6,509,811 bp) with 5-bp overlap (ATAGA) (Fig. 2C). The deletion occured de novo as FISH and

TABLE I. Clinical Manifestations of Reported Cases of 20q11–q12 Deletion

	Calliers' case (4 y, female)	Iqbals' case (2 y, male)	Present case (18 m, male)
General			
Growth retardation	+	+	+
Developmental delay	+	+	+
Autistic behavior	+	+	+
Sensory abnormalities/self-injury	+	+	+
Feeding difficulties	+	+	+
Gastroesophageal reflux	+	+	+
Gastrointestinal abnormalities	+ (Pyloric stenosis)	−	+ (Esophageal hiatus hernia)
Feeding intolerance	+ (Diarrhea, vomiting)	−	−
Dysphagia			+
Food refusal	+		+
Muscle tone	Hypertonia	Normal tone except for difficulty in extending the hips	Normal tone
Hearing loss		+	+
Congenital heart defect	−	−	+
Seizure/epilepsy		−	+
Central nervous system			
Cerebral atrophy	+	+	+
Craniofacial			
Triangular face	+	+	+
Hypertelorism	+	+	+
Hypoplastic alae nasi	+	+	+
Sparse hair	+		+
Down-slanting palpebral fissures	+		+
Long columella	+		+
Short, well-defined philtrum	+		+
Thin lips	+		+
Microretrognathia	+		+
Low-set ears	+		+
Extremities			
Arthrogryposis			+
Preaxial polydactyly			+
Clinodactyly of 5th fingers	+		+
Talipes equinovarus		+	
Talopes valgus			+
Ocular			
Retinal dysplasia			+
Microphthalmia		+	−
Duane anomaly		+	n.d.
Strabismus	+		−
Others			
Genital anomlies		+	−

Shadow indicates common features among three cases. y, year(s); m, month(s); +, positive; −, negative; n.d., not determined.

junction PCRs denied the deletion in parental samples (FISH data not shown and Fig. 2B by PCR using primers A, B, and C [primer B: 5′-AGC TGC TCA AAG TGG GGT ATT CTG G-3′]).

DISCUSSION

In this study, we precisely analyzed the 6.5-Mb deletion at 20q11.2–q12 in a boy, presenting with abnormal hands and feet, retinal dysplasia, and intractable feeding difficulty. Proximal interstitial deletions of 20q11–q12 are very rare. Only two cases have been reported and analyzed either by chromosomal CGH and FISH analysis or BAC array CGH with 1-Mb resolution [Callier et al., 2006; Iqbal and Al-Owain, 2007]. Clinical features are presented in Figure 1 and summarized in Table I. Three deletions are overlapping and the shortest region of overlap is from 20q11.22 to q11.23 (Fig. 3). Common clinical features among three cases are

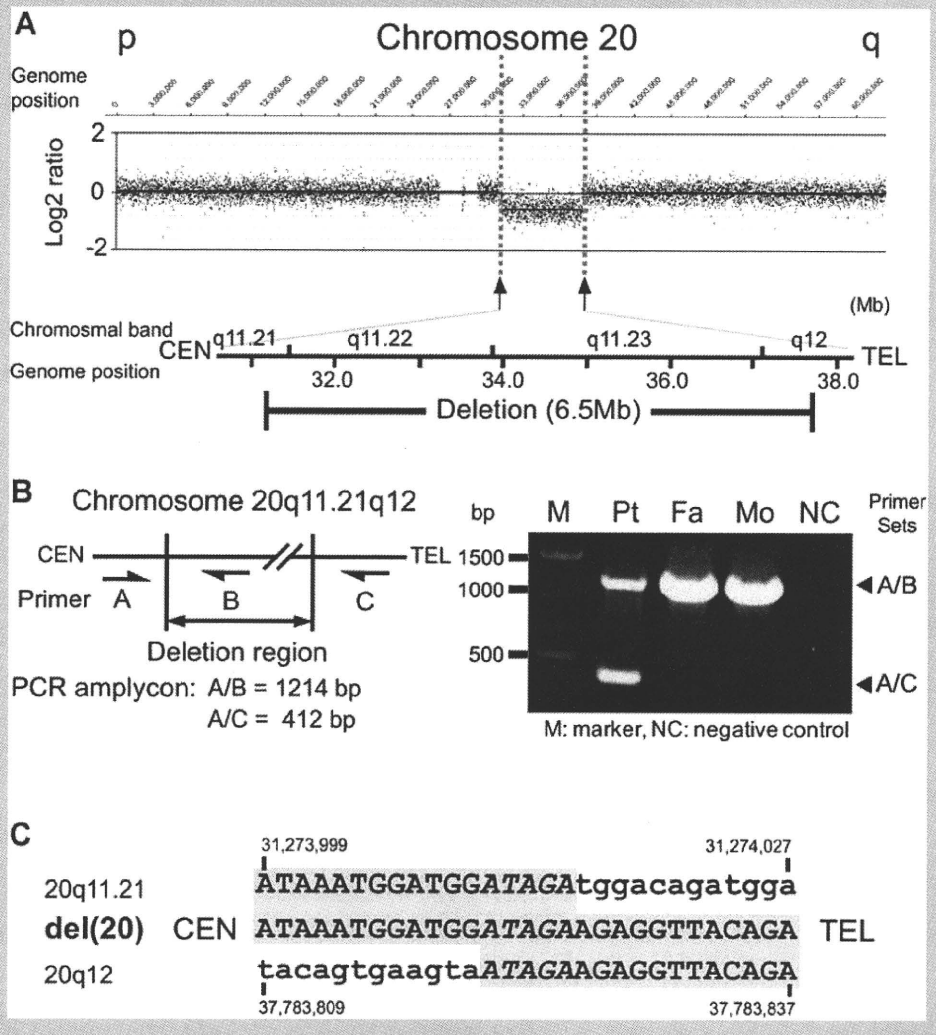

FIG. 2. Analysis of the 20q11.21–q12 deletion. A: High-resolution SNP array revealed the 6.5-Mb deletion at 20q11.21–q12. In the upper part, *Y* and *X* axes indicate probe signal intensity (log 2 ratio) and probe position in chromosome 20, respectively, and in the lower, chromosomal bands together with location of the deletion are shown. B: PCR system (left) to delineate the deletion and its result (right). C: Deletion junction sequence. Upper and lower sequences are normal ones around at proximal [20q11.21] and distal [20q12] deletion breakpoints, respectively. Middle shows the deletion junction in the patient. Gray shadow indicates matched sequences.

growth/developmental retardation, intractable feeding difficulties with GER, cerebral atrophy, and dysmorphic face including triangular face, hypertelorism, and hypoplastic alae nasi. In addition, two out of three patients shared many other facial dysmorphism including sparse hair, downslanting palpebral fissures, long columella, short and well-defined philtrum, thin lips, microretrognathia, and low-set ears. These findings suggest that the 20q11.22–q11.23 deletion can be a recognizable microdeletion syndrome. In addition, unique findings of hands and feet abnormalities as well as retinal dysplasia were found in our patient.

Intractable feeding difficulties in the three patients, is the largest concern for the family, and are speculated to be caused by combined factors: prolonged dysphagia (in our case), aspiration associated with GER (in all three), upper gastrointestinal tract abnormalties (pyloric stenosis [Callier et al., 2006] or esophageal hiatus hernia in our case), vomiting/diarrhea because of feeding intorerance [Callier et al., 2006], sensory abnormalities (in all), and food refusal (in the Callier et al. and our patient).

According to UCSC genome browser (March 2006 assembly), the 6.5-Mb deleted segment identified in our patient encompasses at least 96 known genes, including nine genes related to human disorders. One of these is growth/differentiation factor-5 (*GDF5*, also known as *CDMP1*). This is a protein which belongs to the GDF-subgroup of BMPs and plays an key regulatory role in embryonic skeletal and joint development. *GDF5* abnormalities are known to cause a variety of different skeletal disorders. Interestingly, Everman et al. [2002] and Yang et al. [2008] indicated that functional *GDF5* haploinsufficiency was the culprit of brachydactyly type C (BDC,

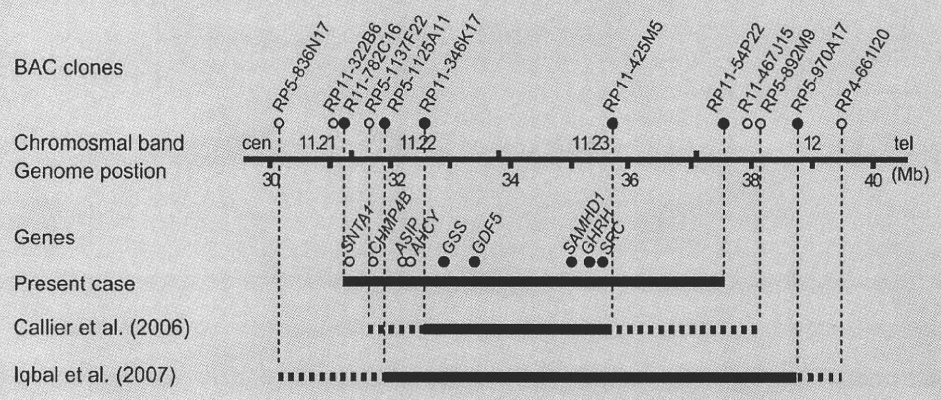

FIG. 3. Shematic presentation of the 20q11–q12 deletions. From top to bottom, BAC clones delineating deletions of all the cases (filled dot: deleted, open dot: not deleted) [Callier et al., 2006; Iqbal and Al-Owain, 2007], chromosomal bands from 20q11.2 to 20q12, genomic position, OMIM genes, and deleted regions of our case and previous ones. Solid and dotted horizontal lines indicate deleted and unconfirmed regions due to the relatively low resolution of the analytical methods.

OMIM #113100) by in vitro studies. As our patient has the *GDF5* haploinsufficiency, he may have the risk for BDC. However, he did not show this manifestation. He did have polydactyly, talipes valgus, and absence of the middle phalanges of the toes, which have been often found in individuals with BDC [Everman et al., 2002; Temtamy and Aglan, 2008]. Our patient did have a fetal akinesia (or hypokinesia) deformation phenotype (FADP). The short neck, hypertelorism, micrognathia, small thorax, postnatal respiratory disturbance, prolonged feeding difficulty, and slender long bone could represent FADP. FADP is a clinically and genetically heterogeneous constellation arising from fetal akinesia or decrease in utero movement due to intrinsic factors including neuropathy, myopathy, and restrictive dermopathy or extrinsic factors that limit fetal movement (e.g., tetragen exposure or fetal crowding) [Witters et al., 2002; Bamshad et al., 2009]. As extrinsic factors (e.g., abnormality of amniotic fluid, fetal crowding, congenital infection, and use of the drug in utero) could not be confirmed in this patient and the arthrogryposis and FADP are accompanied by other organ anomalies and developmental delay, the gene(s) at 20q11.21–q11.23 may be a primary intrinsic cause. Unfortunately, as skeletal malformations in the other two cases having the 20q11.2–q12 deletion were not fully described [Callier et al., 2006; Iqbal and Al-Owain, 2007], it is difficult to discuss the relationship between skeletal features and gene(s) in 20q11.2–q12 deletion.

Retinal dysplasia associated with falciform retinal fold and impaired vision was also noted. Retinal dysplasia is defined as abnormal growth and differentiation of embryonic retina either due to in utero environmental factors such as viral infection, tetragen exposure, retinopathy of prematurity or genetic factors. To our knowledge, this is the first description of retinal dysplasia associated with 20q11.2–q12 deletion.

ACKNOWLEDGMENTS

We are grateful to the patient and his family for their participation and support to this study. Grant-in Aid for Japan Society for the Promotion of Science (JSPS) Fellow (A.N.), Research Grants from the Ministry of Health, Labour and Welfare (N.M.), Grant-in-Aid from the Ministry of Education, Culture, Sports, Science and Technology of Japan (N.M.), and Grant-in-Aid for Scientific Research from JSPS (N.M.).

REFERENCES

Aldred MA, Aftimos S, Hall C, Waters KS, Thakker RV, Trembath RC, Brueton L. 2002. Constitutional deletion of chromosome 20q in two patients affected with albright hereditary osteodystrophy. Am J Med Genet 113:167–172.

Bamshad M, Van Heest AE, Pleasure D. 2009. Arthrogryposis: A review and update. J Bone Joint Surg Am 91:40–46.

Borozdin W, Graham JM Jr, Bohm D, Bamshad MJ, Spranger S, Burke L, Leipoldt M, Kohlhase J. 2007. Multigene deletions on chromosome 20q13.13-q13.2 including SALL4 result in an expanded phenotype of Okihiro syndrome plus developmental delay. Hum Mutat 28:830.

Callier P, Faivre L, Marle N, Thauvin-Robinet C, Sanlaville D, Gosset P, Prieur M, Labenne M, Huet F, Mugneret F. 2006. Major feeding difficulties in the first reported case of interstitial 20q11.22-q12 microdeletion and molecular cytogenetic characterization. Am J Med Genet Part A 140A:1859–1863.

Everman DB, Bartels CF, Yang Y, Yanamandra N, Goodman FR, Mendoza-Londono JR, Savarirayan R, White SM, Graham JM Jr, Gale RP, Svarch E, Newman WG, Kleckers AR, Francomano CA, Govindaiah V, Singh L, Morrison S, Thomas JT, Warman ML. 2002. The mutational spectrum of brachydactyly type C. Am J Med Genet 112:291–296.

Genevieve D, Sanlaville D, Faivre L, Kottler ML, Jambou M, Gosset P, Boustani-Samara D, Pinto G, Ozilou C, Abeguile G, Munnich A, Romana S, Raoul O, Cormier-Daire V, Vekemans M. 2005. Paternal deletion of the GNAS imprinted locus (including Gnasxl) in two girls presenting with severe pre- and post-natal growth retardation and intractable feeding difficulties. Eur J Hum Genet 13:1033–1039.

Iqbal MA, Al-Owain M. 2007. Interstitial del(20)(q11.2q12)—Clinical and molecular cytogenetic characterization. Am J Med Genet Part A 143A:1880–1884.